

Measuring Fairness under Unawareness via Quantification

Alessandro Fabris · Andrea Esuli ·
Alejandro Moreo · Fabrizio Sebastiani

Received: date / Accepted: date

Abstract Models trained by means of supervised learning are increasingly deployed in high-stakes domains, and, when their predictions inform decisions about people, they inevitably impact (positively or negatively) on their lives. As a consequence, those in charge of developing these models must carefully evaluate their impact on different groups of people and ensure that sensitive demographic attributes, such as race or sex, do not result in unfair treatment for members of specific groups. For doing this, awareness of demographic attributes on the part of those evaluating model impacts is fundamental. Unfortunately, the collection of these attributes is often in conflict with industry practices and legislation on data minimization and privacy. For this reason, it may be hard to measure the *group fairness* of trained models, even from within the companies developing them. In this work, we tackle the problem of measuring group fairness under unawareness of sensitive attributes, by using techniques from *quantification*, a supervised learning task concerned with directly providing group-level prevalence estimates (rather than individual-level class labels). We identify five important factors that complicate the estimation of fairness under unawareness and formalize them into five different experimental protocols under which we assess the effectiveness of different estimators of group fairness. We also consider the problem of potential model misuse to infer sensitive attributes at an individual level, and demonstrate that quantification approaches are suitable for decoupling the (desirable) objective of measuring

Alessandro Fabris
Dipartimento di Ingegneria dell'Informazione
Università di Padova
Via Giovanni Gradenigo 6B – 35131 Padova, Italy
E-mail: fabrisal@dei.unipd.it

Andrea Esuli · Alejandro Moreo · Fabrizio Sebastiani
Istituto di Scienza e Tecnologie dell'Informazione
Consiglio Nazionale delle Ricerche
Via Giuseppe Moruzzi 1 – 56124 Pisa, Italy
E-mail: *firstname.lastname*@isti.cnr.it

group fairness from the (undesirable) objective of inferring sensitive attributes of individuals.

Keywords Model Auditing · Group Fairness · Fairness under Unawareness · Quantification

1 Introduction

The widespread adoption of automated decision-making in high-stakes systems has brought about an increased attention to the underlying algorithms and to their effects across sensitive groups. Typically, sensitive groups are subpopulations determined by social and demographic factors, such as race and sex. The unfair treatment of such demographic groups is ruled out by anti-discrimination laws and studied by a growing community of algorithmic fairness researchers. Important works in this space have addressed problems that may arise in the judicial system (Angwin et al., 2016; Larson et al., 2016), in healthcare (Obermeyer et al., 2019), in job search (Geyik et al., 2019), and in computer vision (Buolamwini and Gebru, 2018), just to name a few domains that may be impacted. One common trait of these works is their attention to a careful definition and measurement of *group fairness*, typically viewed in terms of differences in quantities of interest, such as the acceptance rate, recall, or accuracy, across the salient subpopulations. According to popular definitions of fairness, large such differences correspond to low fairness on the part of the algorithms.

Unfortunately, sensitive demographic data, such as the race and sex of users, is often hard to obtain, for various reasons. There are several barriers to demographic data procurement which make measurement of fairness non-trivial even for the company that is developing and deploying a model. Legislation plays a major role in this, forbidding the collection of sensitive attributes in some domains (Bogen et al., 2020). Even in the absence of explicit prohibition, privacy-by-design standards and a data minimization ethos push companies in the direction of avoiding the collection of sensitive attributes from their customers. Similarly, the prospect of negative media coverage is a clear concern, so companies often err on the side of caution and inaction (Andrus et al., 2021). For these reasons, in a recent survey of industry practitioners, a majority of respondents stated that the availability of tools supporting fairness auditing without access to individual-level demographics would be very useful (Holstein et al., 2019). In other words, the problem of *measuring algorithmic fairness under unawareness of sensitive attributes* is pressing, and requires ad-hoc solutions.

In the algorithmic fairness literature, much work has been done to propose techniques directly aimed at improving the fairness of a model (Donini et al., 2018; Hashimoto et al., 2018; He et al., 2020; Zafar et al., 2017). Comparably little attention, though, has been devoted to the problem of reliably measuring fairness. This represents an important and rather overlooked preliminary step to enforcing fairness and making algorithms more equitable across groups.

More recent works have studied non-ideal conditions, such as noisy or missing group labels (Awasthi et al., 2020; Chen et al., 2019) and non-iid samples (Singh et al., 2021), showing that naïve fairness-enhancing algorithms may actually make a model *less* fair (Mehrotra and Celis, 2021).

In this work, we tackle the problem of measuring algorithmic fairness under unawareness of sensitive attributes, by using techniques from *quantification* (González et al., 2017), a supervised learning task concerned with estimating, rather than the class labels of individual data points, the class prevalence values for sets (usually referred to as “samples”) of such data points. This is precisely the goal of practitioners looking to measure fairness under unawareness of sensitive attributes. When auditing an algorithm for group fairness, the aim is not the development of a model that is accurate for individual predictions (i.e., classification), which may be misused to infer people’s demographics, such as a user’s race, and may thus lead to the inappropriate and non-consensual utilization of this information. Rather, the central interest of fairness audits is the reliable estimation of group-level quantities (i.e., quantification), such as the prevalence of women among the instances to which a certain class has been assigned by the model.

We consider several methods that have been proposed in the quantification literature and assess their suitability for estimating the fairness of a classifier under unawareness of sensitive attributes. More precisely, we adapt quantification approaches to measure a classifier’s *demographic disparity* (Barocas et al., 2019; Wachter et al., 2020), defined as the difference in acceptance rate across relevant subpopulations. Overall, we make the following contributions:

- **Five experimental protocols for five major challenges.** Drawing from the algorithmic fairness literature, we identify five important factors for the problem of estimating fairness under unawareness of sensitive attributes. These factors are based on challenges encountered in real-world applications, including the non-stationarity of processes generating the data, and the variable cardinality of the available samples. For each factor, we define and formalize a precise experimental protocol, through which we compare the performance of quantifiers (i.e., group-level prevalence estimators) generated by six different quantification methods (Sections 5.3–5.7).
- **Adaptation and ablation study.** We demonstrate a simple procedure to adapt and integrate quantification approaches into a wider machine learning pipeline with minimal orchestration effort. We prove the importance of each component through an ablation study (Section 5.8).
- **Quantifying without classifying.** We consider the problem of potential model misuse to maliciously infer demographic characteristics at an individual level, which represents a concern for methods based on proxy attributes. Proxy methods are estimators of sensitive attributes which exploit the correlation between available attributes (e.g., ZIP code) and the sensitive attributes (e.g., race) in order to infer the values of the latter. Through a set of experiments, we demonstrate two methods that yield precise estimates of demographic disparity but poor classification perfor-

mance, thus decoupling the objectives of group-level prevalence estimation and individual-level class label prediction (Section 5.9).

It is worth noting some intrinsic limitations of fairness measures and proxy methods which are also applicable to this work. In essence, proxy methods exploit co-occurrence of membership in a group and display of a given trait, potentially learning, encoding and reinforcing stereotypical associations (Lipton et al., 2018). Even when labels for sensitive attributes are available, these are not all equivalent. Self-reported labels are preferable to avoid external assignment (i.e., inference of sensitive attributes), which may be harmful in itself (Keyes, 2018). More in general, approaches that define sensitive attributes as rigid and fixed categories are limited in that they impose a taxonomy onto people, erasing the needs and experiences of those who do not fit the envisioned prevalent categories (Namaste, 2000). While acknowledging these limitations, we hope our work will help highlight, investigate and mitigate unfavourable outcomes for disadvantaged groups brought about by different automated decision-making systems.

The outline of this work is the following. Section 2 presents the notation employed throughout this manuscript. Section 3 contains a primer on quantification, with emphasis on the approaches considered in this work. Section 4 shows how these approaches can be adapted and integrated to measure demographic disparity. Section 5 presents and discusses our experimental results. Section 6 summarizes the related works. Finally, Section 7 contains concluding remarks, discussing limitations and avenues for future work.

2 Notation

In this paper, we use the following notation, summarized in Table 1. By \mathbf{x} we indicate a data item drawn from a domain \mathcal{X} , encoding a set of non-sensitive attributes (i.e., features) taken by classifiers and quantifiers as an input. We use \mathcal{S} to denote the domain of a sensitive attribute, binarily encoded to $\mathcal{S} = \{0, 1\}$ for ease of exposition, and by s a value that \mathcal{S} may take. By y we indicate a class taking values on a binary domain $\mathcal{Y} = \{\ominus, \oplus\}$, representing the target of a prediction task.¹

Symbol σ denotes a *sample*, i.e., a non-empty set of data points drawn from \mathcal{X} . By $p_\sigma(s)$ we indicate the true prevalence of attribute s in sample σ , while by $\hat{p}_\sigma^q(s)$ we indicate the estimate of this prevalence obtained by means of quantifier q , which we define as a function $q : 2^{\mathcal{X}} \rightarrow [0, 1]$. Since $0 \leq p_\sigma(s) \leq 1$ and $0 \leq \hat{p}_\sigma^q(s) \leq 1$ for all $s \in \mathcal{S}$, and since $\sum_{s \in \mathcal{S}} p_\sigma(s) = \sum_{s \in \mathcal{S}} \hat{p}_\sigma^q(s) = 1$, the $p_\sigma(s)$'s and the $\hat{p}_\sigma^q(s)$'s form two probability distributions across \mathcal{S} .

¹ In this paper we assume the existence of a single binary sensitive attribute \mathcal{S} ; however, there is no loss of generality in this, since everything we say can straightforwardly be extended to the case in which multiple sensitive attributes are present at the same time. Moreover, we focus on the case in which the classifier that we want to audit is a binary one, but the definitions and techniques we employ can be straightforwardly extended to a multiclass setting. See also Footnote 3 on this.

Table 1: Notation for this work.

$\mathbf{x} \in \mathcal{X}$	a data item from domain \mathcal{X} , encoding non-sensitive attributes
$s \in \mathcal{S}$	a sensitive attribute, $\mathcal{S} = \{0, 1\}$
$y \in \mathcal{Y}$	a target variable, $\mathcal{Y} = \{\ominus, \oplus\}$
X, S, Y, \hat{Y}	random variables for non-sensitive and sensitive attributes, target variables and predictions
$h(\mathbf{x})$	$h : \mathcal{X} \rightarrow \mathcal{Y}$ a classifier issuing predictions in \mathcal{Y}
$k(\mathbf{x})$	$k : \mathcal{X} \rightarrow \mathcal{S}$ a classifier issuing predictions for sensitive attribute \mathcal{S}
σ	a sample, i.e., a non-empty set of data points drawn from \mathcal{X}
$p_\sigma(s)$	true prevalence of sensitive attribute s in sample σ
$\hat{p}_\sigma(s)$	estimate of the prevalence of s in σ
$\hat{p}_\sigma^q(s)$	estimate $\hat{p}_\sigma(s)$ obtained via quantifier q
q	$q : 2^{\mathcal{X}} \rightarrow [0, 1]$ a quantifier estimating the prevalence of the positive class of sensitive attribute \mathcal{S} in a given sample
\mathcal{D}_1	training set for $h(\mathbf{x})$, involving $(\mathcal{X}, \mathcal{Y})$
\mathcal{D}_2	auxiliary set, i.e., training set for quantifier q , involving $(\mathcal{X}, \mathcal{S})$
\mathcal{D}_3	deployment set involving \mathcal{X}
$\mathcal{D}_2^\oplus, \mathcal{D}_3^\oplus, \mathcal{D}_3^\ominus$	short for $\mathcal{D}_2^{\hat{Y}=\oplus} = \{(\mathbf{x}_i, s_i) \in \mathcal{D}_2 \mid h(\mathbf{x}_i) = \oplus\}$
$\check{\mathcal{D}}_2, \check{\mathcal{D}}_3, \check{\mathcal{D}}_3^\oplus, \check{\mathcal{D}}_3^\ominus$	analogous sets
$\check{\mathcal{D}}_2^\oplus, \check{\mathcal{D}}_3^\oplus, \check{\mathcal{D}}_3^\ominus$	a modified training set, derived from \mathcal{D}_1 according to a certain experimental protocol. Protocols are detailed in Sections 5.3–5.7
$\check{\mathcal{D}}_2^\oplus, \check{\mathcal{D}}_3^\oplus, \check{\mathcal{D}}_3^\ominus$	analogous sets

We also introduce random variables X, S, Y, \hat{Y} which denote, respectively, data points from \mathcal{X} , their sensitive attributes, true labels, and predicted labels. By $\Pr(V = v)$ we indicate, as usual, the probability that random variable V takes value v , which we shorten as $\Pr(v)$ when V is clear from context. By $h : \mathcal{X} \rightarrow \mathcal{Y}$ we indicate a binary classifier that assigns classes in \mathcal{Y} to data points; by $k : \mathcal{X} \rightarrow \mathcal{S}$ we instead indicate a binary classifier that assigns sensitive attributes \mathcal{S} to data points (e.g., that predicts if a certain data item \mathbf{x} is “female”). It is worth re-emphasizing that both h and k only use non-sensitive attributes from \mathcal{X} as input variables. For ease of use, we will interchangeably write $h(\mathbf{x}) = y$ or $h_y(\mathbf{x}) = 1$, and $k(\mathbf{x}) = s$ or $k_s(\mathbf{x}) = 1$.

We consider three separate datasets, following the workflow of a realistic machine learning pipeline.

- A *training set* \mathcal{D}_1 for h , $\mathcal{D}_1 = \{(\mathbf{x}_i, y_i) \mid \mathbf{x}_i \in \mathcal{X}, y_i \in \mathcal{Y}\}$, typically of large cardinality. Given the inherent difficulties in demographic data procurement, we expect this dataset to contain no explicit information on the sensitive attributes \mathcal{S} .
- A small *auxiliary set* $\mathcal{D}_2 = \{(\mathbf{x}_i, s_i) \mid \mathbf{x}_i \in \mathcal{X}, s_i \in \mathcal{S}\}$, employed to learn quantifiers for the sensitive attribute. This dataset may originate from a targeted effort, such as interviews (Baker et al., 2005), surveys sent to customers asking for voluntary disclosure of sensitive attributes (Andrus et al., 2021), or other optional means to share demographic information

- (Beutel et al., 2019a,b). Alternatively it could derive from data acquisitions carried out for other purposes (Galdon Clavell et al., 2020). Both \mathcal{D}_1 and \mathcal{D}_2 are in the development domain of our machine learning pipeline.
- A *deployment set* $\mathcal{D}_3 = \{\mathbf{x}_i \mid \mathbf{x}_i \in \mathcal{X}\}$ which emulates the production domain for classifier h , whose demographic parity we aim to measure. Alternatively, acting proactively rather than reactively, \mathcal{D}_3 could also be a held-out test set available at a company for pre-deployment audits (Raji et al., 2020). From the perspective of the estimation task at hand, i.e. estimating the demographic disparity of h , \mathcal{D}_2 represents the quantifiers’ training set, while \mathcal{D}_3 is their test set.

3 Learning to quantify

Quantification (also known as *supervised prevalence estimation*, or *learning to quantify*) is the task of training, by means of supervised learning, a predictor that estimates the relative frequency (also known as *prevalence*, or *prior probability*) of the classes of interest in a sample of unlabelled data points, where the data used to train the predictor are a set of labelled data points; see (González et al., 2017) for a survey of research on quantification.

Quantification can be trivially solved via classification, i.e., by classifying all the unlabelled data points by means of a standard classifier and counting the data points that have been assigned to a given class. However, it has unequivocally been shown (see e.g., Fernandes Vaz et al. (2019); Forman (2008); González et al. (2017); González-Castro et al. (2013); Moreo and Sebastiani (2021b)) that solving quantification by means of this *Classify-and-Count* (CC) method is suboptimal in terms of accuracy, and that more accurate quantification methods exist. The reason behind this is the fact that many applicative scenarios suffer from *distribution shift*, the phenomenon according to which the class prevalence values in the training set may substantially differ from the class prevalence values in the unlabelled data that one needs to issue predictions for (Moreno-Torres et al., 2012). The presence of distribution shift means that the well-known IID assumption, on which most learning algorithms for training classifiers are based, does not hold; in turn, this means that CC will perform suboptimally on scenarios that exhibit distribution shift, and that the higher the amount of shift, the worse we can expect CC to perform.

A plethora of quantification methods have been defined in the literature. In the experiments presented in this paper, we compare six such methods, which we briefly present in this section. One of them is the trivial CC baseline; we have chosen the other five methods over other contenders as they are simple and proven, and because some of them (especially methods ACC, PACC, SLD, and HDy – see below) have shown top-notch performance in recent comparative tests run in other domains (Moreo and Sebastiani, 2021a,b).

An obvious way to solve quantification is, as hinted above, by aggregating the scores assigned by a classifier to the unlabelled items. Such methods can use a standard, “hard” classifier (i.e., a classifier $h_{\oplus} : \mathcal{X} \rightarrow \{0, 1\}$ that outputs

Boolean decisions regarding membership to class \oplus or a “soft” classifier (i.e., a classifier $s_{\oplus} : \mathcal{X} \rightarrow [0, 1]$ that outputs posterior probabilities $\Pr(\oplus|\mathbf{x})$, representing the probability that the classifier attributes to the fact that \mathbf{x} belongs to class \oplus).² Of course, $\Pr(\ominus|\mathbf{x}) = (1 - \Pr(\oplus|\mathbf{x}))$. The (trivial) *classify and count* (**CC**) quantifier then comes down to computing

$$\hat{p}_{\sigma}^{\text{CC}}(\oplus) = \frac{\sum_{\mathbf{x} \in \sigma} h_{\oplus}(\mathbf{x})}{|\sigma|} \quad (1)$$

while the *probabilistic classify and count* quantifier (**PCC**) (Bella et al., 2010) is defined by

$$\hat{p}_{\sigma}^{\text{PCC}}(\oplus) = \frac{\sum_{\mathbf{x} \in \sigma} s_{\oplus}(\mathbf{x})}{|\sigma|} \quad (2)$$

Of course, for any quantification method q we have $\hat{p}_{\sigma}^q(\ominus) = (1 - \hat{p}_{\sigma}^q(\oplus))$.

A popular quantification method consists of applying an *adjustment* to the prevalence $\hat{p}_{\sigma}(\oplus)$ estimated via “Classify and Count”. It is easy to check that, in the binary case, the true prevalence $p_{\sigma}(\oplus)$ and the estimated prevalence $\hat{p}_{\sigma}(\oplus)$ are such that

$$p_{\sigma}(\oplus) = \frac{\hat{p}_{\sigma}^{\text{CC}}(\oplus) - fpr_h}{tpr_h - fpr_h} \quad (3)$$

where tpr_h and fpr_h stand for the *true positive rate* and *false positive rate* of the classifier h_{\oplus} used to obtain $\hat{p}_{\sigma}^{\text{CC}}$. The values of tpr_h and fpr_h are unknown, but can be estimated via k -fold cross-validation on the training data. In the binary case, this comes down to using the results $h_{\oplus}(\mathbf{x})$ obtained in the k -fold cross-validation (i.e., \mathbf{x} ranges on the training items) in equations

$$t\hat{p}r_h = \frac{\sum_{\mathbf{x} \in \oplus} h_{\oplus}(\mathbf{x})}{|\{\mathbf{x} \in \oplus\}|} \quad f\hat{p}r_h = \frac{\sum_{\mathbf{x} \in \ominus} h_{\oplus}(\mathbf{x})}{|\{\mathbf{x} \in \ominus\}|}, \quad (4)$$

where by $\{\mathbf{x} \in \oplus\}$ (resp. $\{\mathbf{x} \in \ominus\}$) we denote the set of positive (resp. negative) instances in our training set. We obtain estimates of $p_{\sigma}^{\text{ACC}}(\oplus)$, which define the *adjusted classify and count* method (**ACC**) (Forman, 2008) by replacing tpr_h and fpr_h in Equation 3 with the estimates of Equation 4, i.e.,

$$\hat{p}_{\sigma}^{\text{ACC}}(\oplus) = \frac{\hat{p}_{\sigma}^{\text{CC}}(\oplus) - \hat{f}pr_h}{\hat{t}pr_h - \hat{f}pr_h} \quad (5)$$

If the soft classifier $s_{\oplus}(\mathbf{x})$ is used in place of $h_{\oplus}(\mathbf{x})$, analogues of $\hat{t}pr_h$ and $\hat{f}pr_h$ from Equation 4 can be defined as

$$t\hat{p}r_s = \frac{\sum_{\mathbf{x} \in \oplus} s_{\oplus}(\mathbf{x})}{|\{\mathbf{x} \in \oplus\}|} \quad f\hat{p}r_s = \frac{\sum_{\mathbf{x} \in \ominus} s_{\oplus}(\mathbf{x})}{|\{\mathbf{x} \in \ominus\}|} \quad (6)$$

² While in this work quantifiers are used to estimate the prevalence of sensitive attribute \mathcal{S} , in this section, we present quantification approaches targeting a generic variable \mathcal{Y} , as typical in the literature. Similarly, the hard classifier h in this section should not be confused with the one introduced in Section 2. The notational overlap is limited to the current section, where we follow the typical machine learning conventions in presenting the supervised task of quantification.

We obtain $p_{\sigma}^{\text{PACC}}(\oplus)$ estimates, which define the *probabilistic adjusted classify and count* method (**PACC**) (Bella et al., 2010), by replacing all factors in the right-hand side of Equation 5 with their “soft” counterparts from Equations 2 and 6, i.e.,

$$\hat{p}_{\sigma}^{\text{PACC}}(\oplus) = \frac{\hat{p}_{\sigma}^{\text{PCC}}(\oplus) - \hat{fpr}_s}{\hat{tpr}_s - \hat{fpr}_s} \quad (7)$$

A further method is the one proposed in (Saerens et al., 2002) (which we here call **SLD**, from the names of its proposers), which consists of training a probabilistic classifier and then using the EM algorithm (i) to update (in an iterative, mutually recursive way) the posterior probabilities that the classifier returns, and (ii) to re-estimate the class prevalence values of the test set until convergence.

Lastly, we consider **HDy** (González-Castro et al., 2013), a probabilistic binary quantification method that views quantification as the problem of minimising the divergence (measured in terms of the Hellinger Distance) between two cumulative distributions of posterior probabilities returned by the classifier, one coming from the unlabelled examples and the other coming from a validation set. HDy looks for the mixture parameter α that best fits the validation distribution (consisting of a mixture of a “positive” and a “negative” distribution) to the unlabelled distribution, and returns α as the estimated prevalence of the positive class.³

4 Using quantification to measure fairness under unawareness of sensitive attributes

We adapt the above quantification approaches for estimating a classifier’s fairness. We define classifier fairness in terms of *demographic parity* (also called *statistical parity* (Dwork et al., 2012) or *independence* (Barocas et al., 2019)), and, in particular, of a flavour of demographic parity based on the distribution of sensitive attribute \mathcal{S} conditional on the prediction of the classifier, as proposed in (Wachter et al., 2020) (see also (Amazon, 2021)). We call our estimand the *demographic disparity* of classifier $h : \mathcal{X} \rightarrow \mathcal{Y}$ for attribute value s , and define it as

$$\Delta(s) = \Pr(S = s | \hat{Y} = \ominus) - \Pr(S = s | \hat{Y} = \oplus) \quad (8)$$

or, more concisely,

$$\Delta(s) = \Pr(s | \ominus) - \Pr(s | \oplus) \quad (9)$$

³ All the above methods except HDy admit straightforward extensions from the binary case to the single-label multiclass case (see Moreo and Sebastiani (2021b)). HDy is a method for binary quantification only, but it can be adapted to the single-label multiclass scenario by training a binary quantifier for each class in one-vs-all fashion, estimating the prevalence of each class independently of the others, and normalizing the obtained prevalence values so that they sum up to 1. In this paper, we are not concerned with the single-class multilabel case since in our experiments we consider sensitive attributes s which range on two values only; however, the above considerations would be useful for applying our approach to non-binary attributes.

It is worth reemphasizing that the sensitive attribute \mathcal{S} does *not* belong to the set of attributes \mathcal{X} which generate the feature space on which classifier h operates (in other words, when training h we are *unaware* of \mathcal{S}). Demographic disparity measures whether the prevalence of the sensitive attribute in the group assigned to the positive class is the same as in the group assigned to the negative class; a value $\Delta(s) = 0$ indicates maximum fairness, while values of $\Delta(s) = -1$ or $\Delta(s) = +1$ indicate minimum fairness, with the sign of $\Delta(s)$ indicating whether, for $S = s$, the classifier is biased towards the \oplus class or the \ominus class, respectively.

Example 1 Assume that \mathcal{S} stands for “sex”, s for “female”, and that the classifier is in charge of recommending loan applicants for acceptance, classifying them as “grant” (\oplus) or “deny” (\ominus). For simplicity, let us assume the outcome of the classifier to directly translate into a decision without human supervision. The bank might want to check that the fraction of females out of the total number of loan recipients is approximately the same as the fraction of females out of the total number of applicants who are denied the loan. In other words, the bank might want $\Delta(s)$ to be close to 0. Of course, if the bank is aware of the sex of each applicant, this constraint is very easy to check and, potentially, enforce. If the bank is unaware of applicants’ sex, as we assume here, the problem is not trivial, and this is where our techniques come in.

In estimating the demographic disparity of h , our focus is on the deployment set where h is supporting the decision-making process. To highlight this fact, we rewrite Equation 9 by making the dependence of $\Delta(s)$ on \mathcal{D}_3 explicit, i.e.,

$$\Delta(s) = p_{\mathcal{D}_3^\ominus}(s) - p_{\mathcal{D}_3^\oplus}(s) \quad (10)$$

where we define

$$\begin{aligned} \mathcal{D}_3^\oplus &= \{\mathbf{x} \in \mathcal{D}_3 \mid h(\mathbf{x}) = \oplus\} \\ \mathcal{D}_3^\ominus &= \{\mathbf{x} \in \mathcal{D}_3 \mid h(\mathbf{x}) = \ominus\} \end{aligned} \quad (11)$$

and where we make explicit the fact that, if a value s that attribute \mathcal{S} can take is viewed as a class, the probabilities $\Pr(s|\ominus)$ and $\Pr(s|\oplus)$ of Equation 9 may be seen as the prevalence values of class s in the two samples \mathcal{D}_3^\oplus and \mathcal{D}_3^\ominus . In other words, measuring demographic disparity is reduced to estimating the prevalence values of class s in the two samples \mathcal{D}_3^\oplus and \mathcal{D}_3^\ominus , i.e., *it can be framed as a task of quantification*.

This approach can be easily integrated into existing machine learning pipelines with little orchestration effort. Below, we summarize the workflow we envision:

1. A classifier $h : \mathcal{X} \rightarrow \mathcal{Y}$ is trained (under unawareness of sensitive attribute \mathcal{S}) on \mathcal{D}_1 and ready for production. The assumption that, at this stage, we are unaware of sensitive attribute \mathcal{S} is due to the inherent difficulties in demographic data procurement already mentioned in Section 1.

2. Classifier h naturally imposes a partition of the auxiliary set \mathcal{D}_2 into $\mathcal{D}_2^\ominus = \{(\mathbf{x}_i, s_i) \in \mathcal{D}_2 \mid h(\mathbf{x}) = \ominus\}$ and $\mathcal{D}_2^\oplus = \{(\mathbf{x}_i, s_i) \in \mathcal{D}_2 \mid h(\mathbf{x}) = \oplus\}$. These two disjoint datasets act as the training sets for the two quantifiers q_\ominus and q_\oplus . Quantifier q_\ominus (or its dual q_\oplus) is trained on \mathcal{D}_2^\ominus (resp., \mathcal{D}_2^\oplus) to estimate the prevalence of data points where $S = s$ among the data points labelled with \ominus (resp., \oplus).
3. Classifier h also imposes a partition of the deployment set \mathcal{D}_3 into $\mathcal{D}_3^\ominus = \{\mathbf{x} \in \mathcal{D}_3 \mid h(\mathbf{x}) = \ominus\}$ and $\mathcal{D}_3^\oplus = \{\mathbf{x} \in \mathcal{D}_3 \mid h(\mathbf{x}) = \oplus\}$. Quantifiers q_\ominus and q_\oplus trained in Step 2 are applied to these datasets to obtain an estimate of the prevalence of s in \mathcal{D}_3^\ominus and \mathcal{D}_3^\oplus . The demographic disparity of h , defined in Equation 8, can thus be estimated as

$$\hat{\Delta}(s) = \hat{p}_{\mathcal{D}_3^\ominus}^{q_\ominus}(s) - \hat{p}_{\mathcal{D}_3^\oplus}^{q_\oplus}(s) \quad (12)$$

where, as we recall from Section 2, $\hat{p}_\sigma^q(s)$ denotes the prevalence of attribute value s in set σ as estimated via quantification method q .

This quantification-based way of tackling demographic disparity is suited for a non-invasive auditing procedure, since it allows unawareness of the sensitive attribute \mathcal{S} in the set \mathcal{D}_1 used for training the classifier h to be audited and in the set \mathcal{D}_3 on which this classifier is going to be deployed; it only requires the availability of an auxiliary data set \mathcal{D}_2 where attribute \mathcal{S} is present. Dataset \mathcal{D}_2 may originate from a targeted effort, such as interviews (Baker et al., 2005), surveys sent to customers asking for voluntary disclosure of sensitive attributes (Andrus et al., 2021), or other optional means to share demographic information (Beutel et al., 2019a,b). Alternatively it could derive from data acquisitions carried out for other purposes (Galdon Clavell et al., 2020).

Additionally, we note that this approach is extremely suitable to situations in which the prevalence of attribute value s in \mathcal{D}_2 is possibly very different from the prevalence of s in the test set \mathcal{D}_3 (a situation that certainly characterizes many operational environments) since the best quantification approaches are robust by construction to distribution drift, as we will show in the next section.

5 Experiments

5.1 General setup

In this section, we carry out an evaluation of different estimators of demographic disparity. We propose five experimental protocols (Sections 5.3–5.7) summarized in Table 2. Each protocol focuses on a single factor of import for the estimation problem, varying the size and mutual shift of the training, auxiliary, and deployment set. Protocol names are in the form **action-characteristic-dataset**, as they act on datasets (\mathcal{D}_1 , \mathcal{D}_2 or \mathcal{D}_3) modifying their characteristics (size or class prevalence) through one of two actions (sampling or label flipping). We investigate the effect of each factor on the performance of six estimators of demographic disparity, keeping the remaining factors constant.

Table 2: Summary of experimental protocols.

Protocol name	Variable	Section
sample-prev-\mathcal{D}_1	joint distribution of (S, Y) in \mathcal{D}_1 , via sampling	§ 5.3
flip-prev-\mathcal{D}_1	joint distribution of (S, Y) in \mathcal{D}_1 , via label flipping	§ 5.4
sample-size-\mathcal{D}_2	size of \mathcal{D}_2 , via sampling	§ 5.5
sample-prev-\mathcal{D}_2	joint distribution of (S, \hat{Y}) in \mathcal{D}_2 , via sampling	§ 5.6
sample-prev-\mathcal{D}_3	joint distribution of (S, \hat{Y}) in \mathcal{D}_3 , via sampling	§ 5.7

Under each experimental protocol, the size or the prevalence of a given dataset is carefully varied based on the protocol definition. For every protocol, we perform an extensive empirical evaluation as follows:

- We compare the performance of each estimation technique on three datasets (Adult, COMPAS, and Credit Card Default). The datasets and respective preprocessing are described in detail in Section 5.2. We focus our discussion on experiments carried out on the Adult dataset, depicted and discussed in depth (Figures 1–8), while experiments on COMPAS and Credit Card Default are summarized numerically (Tables 4–8) and only discussed in detail when peculiar.
- We split a given dataset into $\mathcal{D}_A, \mathcal{D}_B, \mathcal{D}_C$, three stratified subsets of identical size and same distribution over (S, Y) . Five such random splits are performed. To test each estimator under the same conditions, these splits are the same for every method.
- For each split, we permute the role of the stratified subsets $\mathcal{D}_A, \mathcal{D}_B, \mathcal{D}_C$, so that each subset alternatively serves as the training (\mathcal{D}_1), auxiliary (\mathcal{D}_2), or deployment set (\mathcal{D}_3). All (six) such permutations are tested.
- Whenever an experimental protocol requires sampling from a subset, for instance when artificially altering a class prevalence value, we perform 10 different samplings. To perform extensive experiments at a reasonable computational cost, every time an experimental protocol requires changing a dataset \mathcal{D} into a shifted version $\check{\mathcal{D}}$, we also reduce its cardinality to $|\check{\mathcal{D}}| = 500$. Further details and implications of this choice on each experimental protocol are provided in the context of the protocol’s setup (e.g., Section 5.3.1).
- Different learning approaches can be used to train the sensitive attribute classifier k underlying each quantification method. We test Logistic Regression (LR) and Support Vector Machines (SVM).⁴ Sections 5.3–5.7 report results of quantification algorithms wrapped around a LR classifier. Analogous results obtain for SVMs, reported in Appendix A.

⁴ Some among the quantification methods we test in this study require the classifier to output posterior probabilities (as is the case for LR). If a classifier natively outputs classification scores that are not probabilities (as is the case for SVM), the former can be converted into the latter via “probability calibration”; see e.g., (Platt, 2000).

- The classifier h , whose demographic disparity we aim to estimate, is LR trained with balanced class weights (i.e., loss weights inversely proportional to class frequencies).
- To measure the effect of a given factor on the performance of different quantifiers, we report the signed estimation error, derived from Equations 10 and 12 as follows:

$$\begin{aligned} e &= \hat{\Delta}(s) - \Delta(s) \\ &= \left[\hat{p}_{\mathcal{D}_3^\ominus}^{q_\ominus}(s) - \hat{p}_{\mathcal{D}_3^\oplus}^{q_\oplus}(s) \right] - \left[p_{\mathcal{D}_3^\ominus}(s) - p_{\mathcal{D}_3^\oplus}(s) \right] \end{aligned} \quad (13)$$

We summarize the experiments by reporting the Mean Absolute Error (MAE – Equation 14) and Mean Squared Error (MSE – Equation 15), where the mean of errors e_i is computed over multiple experiments E .

$$\text{MAE}(E) = \frac{1}{|E|} \sum_{e_i \in E} |e_i| \quad (14)$$

$$\text{MSE}(E) = \frac{1}{|E|} \sum_{e_i \in E} e_i^2 \quad (15)$$

Overall, our experiments consist of over 700,000 separate estimates of demographic disparity.⁵

The remainder of this section is organized as follows. Section 5.2 presents the chosen datasets and the applied preprocessing. Sections 5.3–5.7 motivate and detail the experimental protocols, reporting the performance of different demographic disparity estimators. Section 5.8 describes an ablation study, aimed at investigating the benefits of training and maintaining multiple class-specific quantifiers rather than a single one. Finally, Section 5.9 shows that good estimators of demographic disparity are not necessarily good at classifying the sensitive attribute at an individual level, so that reliable fairness auditing may be decoupled from this undesirable misuse of the same models.

5.2 Datasets

We perform our experiments on three datasets. We choose Adult and COMPAS, two standard datasets in the algorithmic fairness community, and Credit Card Default (hereafter: CreditCard), which serves as a representative use case for a bank performing a fairness audit of a prediction tool used internally. For each dataset, we standardize the selected features by removing the mean and scaling to unit variance.

Adult.⁶ One of the most popular resources on the UCI Machine Learning Repository, the Adult dataset was created as a collection to benchmark

⁵ Code available at <https://github.com/alessandro-fabris/ql4facct>.

⁶ <https://archive.ics.uci.edu/ml/datasets/adult>

the performance of machine learning algorithms. It was extracted from the March 1994 US Current Population Survey and represents respondents along demographic and socio-economic dimensions, reporting, e.g., their sex, race, educational attainment and occupation. Each instance comes with a binary label, encoding whether their income exceeds \$50,000, which is the target of the associated classification task. We consider “sex” the sensitive attribute \mathcal{S} , with a binary categorization of respondents as “Female” or “Male”. From the non-sensitive attributes \mathcal{X} , we remove “education-num” (a redundant feature), “relationship” (where values “husband” and “wife” are near-perfect predictors of “sex”), and “fnlwgt” (a variable released by the US Census Bureau to encode how representative each instance is of the overall population). Categorical variables are dummy-encoded and instances with missing values (7%) are removed.

COMPAS.⁷ This dataset was curated to audit racial biases in the Correctional Offender Management Profiling for Alternative Sanctions (COMPAS) risk assessment tool, which estimates the likelihood of a defendant becoming a recidivist (Angwin et al., 2016; Larson et al., 2016). The dataset represents defendants who were scored for risk of recidivism by COMPAS in Broward County, Florida between 2013–2014, summarizing their demographics, criminal record, custody and COMPAS scores. We consider the `compas-scores-two-years` subset published by ProPublica on github, consisting of defendants that were observed for two years after screening, for whom a binary recidivism ground truth is available. We follow the standard preprocessing to remove noisy instances (ProPublica, 2016). We focus on “race” as a protected attribute \mathcal{S} , restricting the data to defendants labelled “African-American” or “Caucasian”. Our attributes \mathcal{X} are defendant’s age (“age” - integer), number of juvenile felonies, misdemeanours, and other convictions (“juv_fel_count”, “juv_misd_count”, “juv_other_count” - integer), number of prior crimes (“priors_count” - integer) and degree of current charge (“c_charge_degree” - felony or misdemeanour, dummy-encoded).

CreditCard.⁸ This resource was curated to study automated credit card default prediction, following a wave of defaults in Taiwan. The dataset summarizes the payment history of customers of an important Taiwanese bank, from April to October 2005. Demographics, marital status, and education of customers are also provided, along with amount of given credit and a binary variable encoding the default on payment within the next month, which is the associated prediction task. We consider “SEX” (binarily encoded) the sensitive attribute \mathcal{S} and keep every other variable in \mathcal{X} , preprocessing the categorical ones via dummy-encoding (“EDUCATION”, “MARRIAGE”, “PAY_0”, “PAY_2”, “PAY_3”, “PAY_4”, “PAY_5”, “PAY_6”). Differently from Adult, we keep marital status as its values are not trivial predictors of the sensitive attribute.

⁷ <https://github.com/propublica/compas-analysis>

⁸ <https://archive.ics.uci.edu/ml/datasets/default+of+credit+card+clients>. Note that we discuss variables with the names they are given in the tabular data (xls file), which do not match the ones in the documentation.

A summary of these datasets and related statistics is reported in Table 3.

Table 3: Dataset statistics after preprocessing.

Dataset	#data items	#non-sensitive features	sensitive attribute	$S = 1$	$Pr(S = 1)$	target variable	$Y = \oplus$	$Pr(Y = 1)$
Adult	45,222	84	sex	Male	0.675	income	> 50K	0.248
COMPAS	5,278	6	race	Caucasian	0.398	recidivist	no	0.498
CreditCard	30,000	81	sex	Male	0.396	default	no	0.779

5.3 Protocol **sample-prev- \mathcal{D}_1**

5.3.1 Motivation and setup

In the first experimental protocol, we evaluate the impact of shifts in the training set \mathcal{D}_1 , by drawing different subsets $\tilde{\mathcal{D}}_1$ as we vary $\Pr(Y = S)$.⁹ More specifically, we vary $\Pr(Y = S)$ between 0 and 1 with a step of 0.1. In other words, we sample at random from \mathcal{D}_1 a proportion p of instances (\mathbf{x}_i, s_i, y_i) such that $Y = S$ and a proportion $(1 - p)$ such that $Y \neq S$, with $p \in \{0.0, 0.1, \dots, 0.9, 1.0\}$. It is worth noting that we defined \mathcal{D}_1 , in Section 2, as a training set involving $(\mathcal{X}, \mathcal{Y})$. Here we exploit our knowledge of \mathcal{S} to control the dataset shift between training and test conditions, emulating a biased data collection procedure. Once a training set has been selected, the classifier h is learnt exclusively from non-sensitive attributes \mathcal{X} , completely disregarding the sensitive attribute \mathcal{S} . We choose a limited cardinality $|\tilde{\mathcal{D}}_1| = 500$, which lets us perform multiple repetitions at reasonable computational costs, as outlined in Section 5.1. While this may impact the quality of the classifier h , this aspect is not the central focus of the present work.

This experimental protocol aligns with biased data collection procedures, sometimes referred to as *censored data* (Kallus and Zhou, 2018). Indeed, it is common for the ground truth variable to represent a mere proxy for the actual quantity of interest, with non-trivial sampling effects between the two. For instance, the validity of arrest data as a proxy for offence has been brought into question (Fogliato et al., 2021). Indeed, in this domain, different sources of sampling bias may be in action, such as uneven allocation of police resources across jurisdictions and neighbourhoods (Holmes et al., 2008) and lower levels of cooperation in populations who feel oppressed by law enforcement (Xie and Lauritsen, 2012).

By varying $\Pr(Y = S)$ we are imposing a spurious correlation between Y and S , which may be picked up by the classifier h . In extreme situations, such as when $\Pr(Y = S) \simeq 1$, a classifier h may end up confounding the concepts behind S and Y . In turn, we expect this to unevenly impact the acceptance

⁹ Although Y and S take values from different domains, by $Y = S$ we mean $(Y = \oplus \wedge S = 1) \vee (Y = \ominus \wedge S = 0)$, i.e. a situation where positive outcomes are associated with group $S = 1$ and negative outcomes with group $S = 0$.

```

Input : • Dataset  $\mathcal{D}$  ;
          • Classifier learner CLS;
          • Quantification method Q;
Output: • MAE of the demographic disparity estimates ;
          • MSE of the demographic disparity estimates ;

1  $E \leftarrow \emptyset$  ;
2 for 5 random splits do
3    $\mathcal{D}_A, \mathcal{D}_B, \mathcal{D}_C \leftarrow \text{split\_stratify}(\mathcal{D})$  ;
4   for  $\mathcal{D}_1, \mathcal{D}_2, \mathcal{D}_3 \in \text{permutations}(\mathcal{D}_A, \mathcal{D}_B, \mathcal{D}_C)$  do
5     for 10 repeats do
6       for  $p \in \{0.0, 0.1, \dots, 0.9, 1.0\}$  do
7         /* Generate samples from  $\mathcal{D}_1$  at desired prevalence */
8          $\check{\mathcal{D}}_1 \sim \mathcal{D}_1$  with  $P(Y = S) = p$  and  $|\check{\mathcal{D}}_1| = 500$  ;
9         /* Learn a classifier  $h : X \rightarrow Y$  */
10         $h \leftarrow \text{CLS.fit}(\check{\mathcal{D}}_1)$  ;
11        /* Learn quantifiers  $q_y : 2^{\mathcal{X}} \rightarrow [0, 1]$  */
12         $\mathcal{D}_2^{\ominus} \leftarrow \{(\mathbf{x}_i, s_i) \in \mathcal{D}_2 \mid h(\mathbf{x}_i) = \ominus\}$  ;
13         $\mathcal{D}_2^{\oplus} \leftarrow \{(\mathbf{x}_i, s_i) \in \mathcal{D}_2 \mid h(\mathbf{x}_i) = \oplus\}$  ;
14         $q_{\ominus} \leftarrow \text{Q.fit}(\mathcal{D}_2^{\ominus})$  ;
15         $q_{\oplus} \leftarrow \text{Q.fit}(\mathcal{D}_2^{\oplus})$  ;
16        /* Use quantifiers to estimate demographic prevalence */
17         $\mathcal{D}_3^{\ominus} \leftarrow \{\mathbf{x}_i \in \mathcal{D}_3 \mid h(\mathbf{x}_i) = \ominus\}$  ;
18         $\mathcal{D}_3^{\oplus} \leftarrow \{\mathbf{x}_i \in \mathcal{D}_3 \mid h(\mathbf{x}_i) = \oplus\}$  ;
19         $\hat{p}_{\mathcal{D}_3^{\ominus}}^{q_{\ominus}}(s) \leftarrow q_{\ominus}(\mathcal{D}_3^{\ominus})$  ;
20         $\hat{p}_{\mathcal{D}_3^{\oplus}}^{q_{\oplus}}(s) \leftarrow q_{\oplus}(\mathcal{D}_3^{\oplus})$  ;
21        /* Compute the signed error of the demographic disparity
           estimate */
22         $e = \left[ \hat{p}_{\mathcal{D}_3^{\ominus}}^{q_{\ominus}}(s) - \hat{p}_{\mathcal{D}_3^{\oplus}}^{q_{\oplus}}(s) \right] - \left[ p_{\mathcal{D}_3^{\ominus}}(s) - p_{\mathcal{D}_3^{\oplus}}(s) \right]$  ;
23         $E \leftarrow E \cup \{e\}$ 
24      end
25    end
26  end
27 end
28  $\text{mae} \leftarrow \text{MAE}(E)$  ;
29  $\text{mse} \leftarrow \text{MSE}(E)$  ;
30 return mae, mse

```

Pseudocode 1: Protocol **sample- $\text{prev-}\mathcal{D}_1$** .

rates for the two demographic groups, effectively changing the demographic disparity of h , i.e., our estimand $\Delta(s)$.

Pseudocode 1 describes the main steps to implement Protocol **sample- $\text{prev-}\mathcal{D}_1$** . The pale red region highlights the part of the experimental protocol that is specific to Protocol **sample- $\text{prev-}\mathcal{D}_1$** ; the rest is common to all experimental protocols.

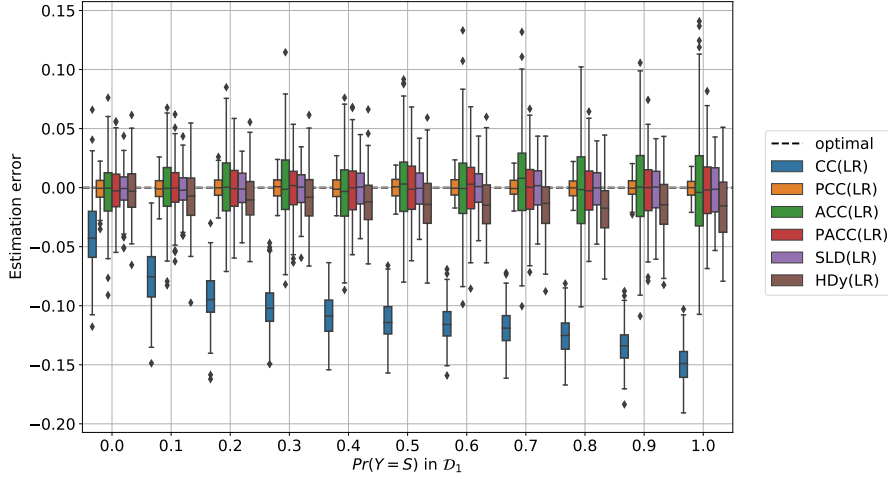


Fig. 1: Protocol **sample-prev- \mathcal{D}_1** on the Adult dataset. Distribution of the estimation error (y axis) as $\check{\mathcal{D}}_1$ is sampled with a given $\Pr(Y = S)$ (x axis). Each boxplot summarizes the results of 5 random splits, 6 role permutations and 10 samplings of $\check{\mathcal{D}}_1$.

5.3.2 Results

Figure 1 reports the performance of CC, PCC, ACC, PACC, SLD, and HDy on the Adult dataset under the **sample-prev- \mathcal{D}_1** experimental protocol. The y axis depicts the estimation error (Equation 13), as we vary $\Pr(Y = S)$ along the x axis. Each boxplot summarizes the results of 5 random splits, 6 role permutations, and 10 samplings of $\check{\mathcal{D}}_1$, for a total of 300 repetitions for each combination of 6 methods and 11 values which vary on the x axis.

Each quantification approach outperforms vanilla CC, which constantly underestimates the demographic disparity of the classifier h , i.e., its estimate is lower than the ground truth value, so that $\hat{\Delta}^{\text{CC}}(s) < \Delta(s)$. ACC, PACC, SLD and HDy display a negligible bias and a reliable estimate of demographic disparity. The absolute error for these techniques is always below 0.1, except for a few outliers.

PCC stands out as a strong performer, with low bias and low variance. This is due to the fact that, under this experimental protocol, no shift is present between the auxiliary set \mathcal{D}_2 , where quantifiers are learnt, and the test set \mathcal{D}_3 , where they are tested. As the current protocol focuses on shifts in the training set, \mathcal{D}_2 and \mathcal{D}_3 remain stratified subsets of the Adult dataset, with

Table 4: Protocol **sample-prev- \mathcal{D}_1** . The first and second columns indicate the values of MAE and MSE (lower is better) obtained in our experiments, while the third and fourth columns indicate the probability that the Absolute Error (AE) falls below 0.1 and 0.2 (higher is better), respectively.

Boldface indicates the best method for a given dataset and metric.

Superscripts \dagger and \ddagger denote the methods (if any) whose error scores (MAE, MSE) are *not* statistically significantly different from the best ones according to a paired sample, two-tailed t-test at different confidence levels: symbol \dagger indicates $0.001 < p\text{-value} < 0.05$, while symbol \ddagger indicates $0.05 \leq p\text{-value}$.

The absence of any such symbol indicates $p\text{-value} \leq 0.001$ (i.e., that the performance of the method is statistically significantly different from that of the best method).

		MAE	MSE	$P(\text{AE} < 0.1)$	$P(\text{AE} < 0.2)$
Adult	CC(LR)	0.107 \pm 0.033	0.013 \pm 0.006	0.343	1.000
	PCC(LR)	0.007 \pm 0.005	0.000 \pm 0.000	1.000	1.000
	ACC(LR)	0.027 \pm 0.021	0.001 \pm 0.002	0.994	1.000
	PACC(LR)	0.019 \pm 0.014	0.001 \pm 0.001	1.000	1.000
	SLD(LR)	0.015 \pm 0.010	0.000 \pm 0.000	1.000	1.000
	HDy(LR)	0.021 \pm 0.015	0.001 \pm 0.001	1.000	1.000
COMPAS	CC(LR)	0.201 \pm 0.070	0.045 \pm 0.030	0.061	0.518
	PCC(LR)	0.026 \pm 0.018	0.001 \pm 0.001	1.000	1.000
	ACC(LR)	0.287 \pm 0.204	0.124 \pm 0.167	0.188	0.389
	PACC(LR)	0.180 \pm 0.152	0.055 \pm 0.097	0.363	0.650
	SLD(LR)	0.108 \pm 0.080	0.018 \pm 0.025	0.546	0.858
	HDy(LR)	0.093 \pm 0.070	0.014 \pm 0.019	0.608	0.914
CreditCard	CC(LR)	0.068 \pm 0.043	0.006 \pm 0.007	0.788	0.996
	PCC(LR)	0.011 \pm 0.008	0.000 \pm 0.000	1.000	1.000
	ACC(LR)	0.194 \pm 0.152	0.061 \pm 0.091	0.326	0.593
	PACC(LR)	0.140 \pm 0.111	0.032 \pm 0.048	0.448	0.744
	SLD(LR)	0.052 \pm 0.041	0.004 \pm 0.007	0.872	0.996
	HDy(LR)	0.067 \pm 0.050	0.007 \pm 0.010	0.767	0.985

identical distribution over (S, Y) . This in turn favours PCC, which relies on the posterior probabilities of its classifier k being well calibrated on \mathcal{D}_3 .¹⁰

Results for the COMPAS and CreditCard datasets are reported in Table 4, along with a summary of results for the Adult dataset we just discussed. Columns labelled MAE and MSE report the Mean Absolute Error and Mean Squared Error of each technique, as defined in Equations (14) and (15). The last two columns report the frequency with which the absolute error is below 0.1 (second-to-last column) and 0.2 (last column) across the entire experimental protocol. The trends we discussed also hold for COMPAS and CreditCard.

¹⁰ Posterior probabilities $Pr(s|\mathbf{x})$ are said to be *well calibrated* when, given a sample σ drawn from \mathcal{X}

$$\lim_{|\sigma| \rightarrow \infty} \frac{|\{\mathbf{x} \in s \mid Pr(s|\mathbf{x}) = \alpha\}|}{|\{\mathbf{x} \in \sigma \mid Pr(s|\mathbf{x}) = \alpha\}|} = \alpha.$$

i.e., when for big enough samples, α approximates the true proportion of data items belonging to class s among all data items for which $Pr(s|\mathbf{x}) = \alpha$.

Most notably, both datasets appear to provide a harder setting for the inference of the sensitive attribute \mathcal{S} from the non-sensitive attributes \mathcal{X} , as shown by higher MAE and MSE, which, for instance, increase by one order of magnitude for SLD and PACC moving from Adult to COMPAS.

5.4 Protocol **flip-prev- \mathcal{D}_1**

5.4.1 *Motivation and setup*

Certain biases in the training set resulting from domain-specific practices, such as the use of arrest as a substitute for offence, may be modelled as either a selection bias (Fogliato et al., 2021) or a label bias distorting the ground truth variable Y (Fogliato et al., 2020). With this experimental protocol, we impose the latter bias by actively flipping some ground truth labels Y in \mathcal{D}_1 based on their sensitive attribute. Similarly to **sample-prev- \mathcal{D}_1** , this protocol achieves a given association between the target Y and sensitive variable S in the training set \mathcal{D}_1 . However, instead of sampling, it does so by flipping the Y label of some data points. More specifically, we impose $\Pr(Y = \ominus | S = 0) = \Pr(Y = \oplus | S = 1) = p$ and let p take values across eleven evenly spaced values between 0 and 1. For every value of p , we firstly sample a random subset $\tilde{\mathcal{D}}_1$ of the training set with cardinality 500. Next, we actively flip some Y labels in both demographic groups, until both $\Pr(Y = \ominus | S = 0)$ and $\Pr(Y = \oplus | S = 1)$ reach a desired value of $p \in \{0.0, 0.1, \dots, 0.9, 1.0\}$. Finally, we train a classifier h on the attributes \mathcal{X} and modified ground truth Y of $\tilde{\mathcal{D}}_1$.

This experimental protocol is compatible with settings where the training data captures a distorted ground truth due to systematic biases and group-dependent annotation accuracy (Wang et al., 2021). As an example, the quality of medical diagnoses can depend on race, sex and socio-economical status (Gianfrancesco et al., 2018). Moreover, health care expenditures have been used as a proxy to train an algorithm deployed nationwide in the US to estimate patients’ health care needs, resulting in systematic underestimation of the needs of black patients (Obermeyer et al., 2019). In the hiring domain, employer response rates to resumes have been found to vary with the perceived ethnic origin of an applicant’s name (Bertrand and Mullainathan, 2004). Finally, the gender gap in mathematical performance, while negligible in elementary school, has been found to increase with age (Lindberg et al., 2010), possibly due to gender stereotypes arising in this domain from an early age (Cvencek et al., 2011) and to the prescriptive nature of these stereotypes (Ellemers, 2018; Nosek et al., 2002). These are all examples where the “ground truth” associated with a dataset is distorted to the disadvantage of a sensitive demographic group.

Similarly to Section 5.3, we expect this experimental protocol to bring about sizeable variations in the demographic disparity of classifier h due to the strong correlation we are imposing between S and Y via label flipping.

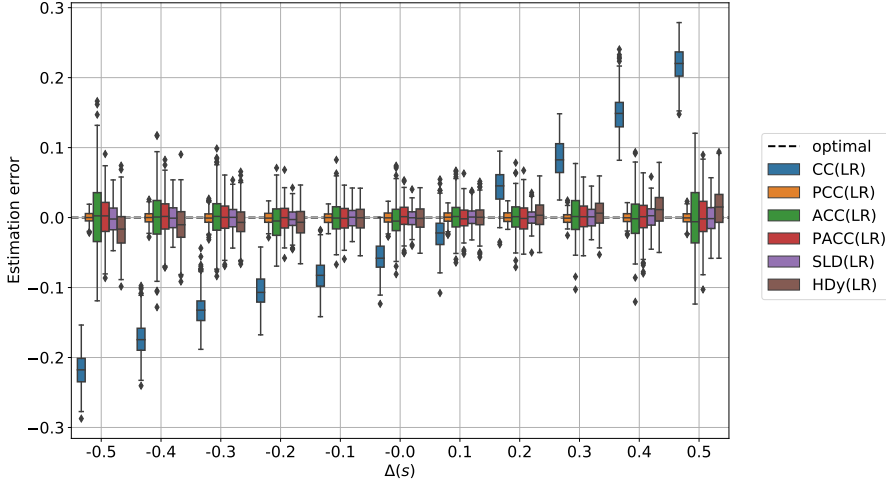


Fig. 2: Protocol **flip-prev- \mathcal{D}_1** on the Adult dataset. Distribution of the estimation error (y axis) as $\Delta(s)$ varies (x axis).

The pseudocode describing this protocol is essentially the same as in Pseudocode 1, simply replacing the sampling in line 8 with the label flipping procedure described above; we hence omit it for the sake of conciseness.

5.4.2 Results

Figure 2 illustrates the key trends brought about by this experimental protocol on the Adult dataset. A clear trend is visible along the x axis, which reports the true demographic disparity $\Delta(s)$ for the classifier h (Equation 10), quantized with a step of 0.1. We choose to depict the true demographic disparity on the x axis as it is the estimand, hence a quantity of interest by definition. The error incurred by CC displays a linear trend that goes from severe under-estimation (for low values of the x axis) to severe over-estimation (for large values of the x axis). In other words, the (signed) estimation error increases with the true demographic disparity of the classifier h , a phenomenon also noticed by Chen et al. (2019).

All remaining approaches compensate for this weakness and display a good estimation error: PCC, ACC, PACC, SLD, HDy have low variance and a median estimation error of zero across different values of the estimand. PCC stands out as particularly effective, which, just like for protocol **sample-prev- \mathcal{D}_1** , can be explained with a complete absence of shift between \mathcal{D}_2 and \mathcal{D}_3 , which makes the posteriors of the underlying classifier k reliable during inference.

As summarized in Table 5, similar trends obtain for the COMPAS dataset, albeit with worse average performance, already noticed in Section 5.3. A notable result on CreditCard is the solid performance of Classify-and-Count. We notice that, on CreditCard, the entire range of biased training sets $\tilde{\mathcal{D}}_1$

Table 5: Protocol **flip-prev- \mathcal{D}_1** .

		MAE	MSE	$P(\text{AE} < 0.1)$	$P(\text{AE} < 0.2)$
Adult	CC(LR)	0.131 \pm 0.066	0.021 \pm 0.018	0.341	0.830
	PCC(LR)	0.007 \pm 0.005	0.000 \pm 0.000	1.000	1.000
	ACC(LR)	0.027 \pm 0.022	0.001 \pm 0.002	0.989	1.000
	PACC(LR)	0.019 \pm 0.015	0.001 \pm 0.001	1.000	1.000
	SLD(LR)	0.014 \pm 0.010	0.000 \pm 0.000	1.000	1.000
	HDy(LR)	0.020 \pm 0.016	0.001 \pm 0.001	1.000	1.000
COMPAS	CC(LR)	0.247 \pm 0.091	0.070 \pm 0.047	0.051	0.297
	PCC(LR)	0.026 \pm 0.019	0.001 \pm 0.001	1.000	1.000
	ACC(LR)	0.288 \pm 0.203	0.124 \pm 0.170	0.186	0.385
	PACC(LR)	0.177 \pm 0.142	0.052 \pm 0.083	0.347	0.652
	SLD(LR)	0.109 \pm 0.081	0.018 \pm 0.025	0.541	0.857
	HDy(LR)	0.090 \pm 0.070	0.013 \pm 0.019	0.625	0.920
CreditCard	CC(LR)	0.055 \pm 0.038	0.005 \pm 0.005	0.859	1.000
	PCC(LR)	0.011 \pm 0.008	0.000 \pm 0.000	1.000	1.000
	ACC(LR)	0.197 \pm 0.154	0.063 \pm 0.094	0.326	0.588
	PACC(LR)	0.136 \pm 0.106	0.030 \pm 0.046	0.450	0.764
	SLD(LR)	0.056 \pm 0.042	0.005 \pm 0.007	0.842	0.995
	HDy(LR)	0.069 \pm 0.053	0.008 \pm 0.011	0.753	0.977

imposed by protocol **flip-prev- \mathcal{D}_1** brings about low variability in the true demographic disparity of classifier h on \mathcal{D}_3 , such that the maximum and minimum values of $\Delta(s)$ across the entire protocol differ by 0.2. This variability is one order of magnitude lower than the one measured on the Adult dataset, where the maximum and minimum values taken by $\Delta(s)$ differ by 1, as per Figure 2, making estimation via Classify-and-Count more challenging on Adult rather than on CreditCard.

5.5 Protocol **sample-size- \mathcal{D}_2**

5.5.1 Motivation and setup

A further factor of interest for the estimation problem is the size of the auxiliary set \mathcal{D}_2 , whose influence is studied in this experimental protocol. Our goal is to understand how low we can go in the small data regime, before degrading the performance of different estimation techniques. We consider subsets $\tilde{\mathcal{D}}_2$ of the auxiliary set, sampling instances uniformly without replacement from it. We let cardinality $|\tilde{\mathcal{D}}_2|$ take five values that are evenly spaced on a log scale, between a minimum sample size $|\tilde{\mathcal{D}}_2|=1,000$ and a maximum size $|\tilde{\mathcal{D}}_2| = |\mathcal{D}_2|$. In other words, we let the cardinality of the auxiliary set take five different values between 1,000 and $|\mathcal{D}_2|$ in a geometric progression. As described in Section 5.1, for each cardinality of the auxiliary set we wish to test, we perform ten samplings over five splits and six permutations, for a total of 300 repetitions per approach per dataset. Pseudocode 2 describes the Protocol **sample-size- \mathcal{D}_2** , with a pale red region highlighting the parts that are specific to this protocol.

This protocol is justified by the well-documented difficulties in demographic data procurement for industry practitioners, which vary depending on domain, company, and other factors of disparate nature (Andrus et al., 2021; Beutel et al., 2019b; Bogen et al., 2020; Galdon Clavell et al., 2020; Holstein et al., 2019). As an example, Galdon Clavell et al. (2020) perform an internal fairness audit of a personalized well-being recommendation app, for which sensitive features are not collected in production, following data minimization principles. However, sensitive features were available from an initial development phase in an auxiliary set, whose size was determined by prior considerations, likely driven by accuracy requirements rather than fairness ones. Furthermore, the collection of sensitive attributes in the US is highly industry-dependent, ranging from mandatory to forbidden, depending on the fragmented regulation applicable in each domain (Bogen et al., 2020). Finally, high quality auxiliary sets may be obtained through optional surveys (Wilson et al., 2021), for which response rates are highly dependent on trust, and can be improved by making the intended use for the data clearer (Andrus et al., 2021).

For these reasons, the cardinality of the auxiliary set \mathcal{D}_2 is an interesting variable in the context of fairness audits. The estimation methods we consider have peculiar data requirements, with diverse purposes (e.g., estimation of true positive rates – *tpr*) and approaches. For this reason, interesting patterns should emerge from this protocol. We expect key trends for the estimation error to vary monotonically with cardinality $|\mathcal{D}_2|$, which is why we let it vary according to a geometric progression.

5.5.2 Results

The estimation error under this experimental protocol on the Adult dataset is depicted in Figure 3, as we vary the cardinality $|\mathcal{D}_2|$ along the x axis. Clearly, the variance for each approach decreases with the size of its training set. Additionally, slight biases may improve, as is the case with HDy. The most striking trend is the unreliability of ACC and PACC (and especially the former) in the small data regime. Indeed, these are adjusted methods, which require splitting the auxiliary set \mathcal{D}_2 into a first subset used for the actual training of a classifier and a second subset used to compute its *tpr* and *fpr* for the adjustment of prevalence estimates, as per Equations (5) and (7).¹¹

Similar results hold for COMPAS and CreditCard, as reported in Table 6. Across the three datasets, PACC and ACC perform quite poorly due to the difficulty in estimating the *tpr* and *fpr* with few labelled data points available

¹¹ Once the estimations for *tpr* and *fpr* have been computed, it would be possible to *retrain* the classifier, using the whole training set (as is customarily done in other areas of machine learning), thus generating a more robust classifier. In this particular case, however, retraining might cause the adjustment of the quantification to become less stable, since the main ingredients of the adjustment (the *tpr* and *fpr*) actually characterize a different classifier. The extent to which this trade-off (more data vs. unstable adjustment) ends up impacting negatively or positively the final computation of the prevalence values is out of scope for this study; we thus avoid retraining in favour of having congruent estimates for the rates.

```

Input : • Dataset  $\mathcal{D}$  ;
          • Classifier learner CLS;
          • Quantification method Q;
Output: • MAE of the demographic disparity estimates ;
          • MSE of the demographic disparity estimates ;

1  $E \leftarrow \emptyset$  ;
2 for 5 random splits do
3    $\mathcal{D}_A, \mathcal{D}_B, \mathcal{D}_C \leftarrow \text{split\_stratify}(\mathcal{D})$  ;
4   for  $\mathcal{D}_1, \mathcal{D}_2, \mathcal{D}_3 \in \text{permutations}(\mathcal{D}_A, \mathcal{D}_B, \mathcal{D}_C)$  do
5     /* Learn a classifier  $h: X \rightarrow Y$  */
6      $h \leftarrow \text{CLS.fit}(\mathcal{D}_1)$  ;
7     for 10 repeats do
8       for size  $s \in \text{logspace}(\text{from: } 1000, \text{to: } |\mathcal{D}_2|, \text{steps: } 5)$  do
9         /* Generate samples from  $\mathcal{D}_2$  at desired size */
10         $\check{\mathcal{D}}_2 \sim \mathcal{D}_2$  with  $|\check{\mathcal{D}}_2| = s$  ;
11        /* Learn quantifiers  $q_y: 2^{\mathcal{X}} \rightarrow [0, 1]$  */
12         $\check{\mathcal{D}}_2^{\ominus} \leftarrow \{(\mathbf{x}_i, s_i) \in \check{\mathcal{D}}_2 \mid h(\mathbf{x}_i) = \ominus\}$  ;
13         $\check{\mathcal{D}}_2^{\oplus} \leftarrow \{(\mathbf{x}_i, s_i) \in \check{\mathcal{D}}_2 \mid h(\mathbf{x}_i) = \oplus\}$  ;
14         $q_{\ominus} \leftarrow \text{Q.fit}(\check{\mathcal{D}}_2^{\ominus})$  ;
15         $q_{\oplus} \leftarrow \text{Q.fit}(\check{\mathcal{D}}_2^{\oplus})$  ;
16        /* Use quantifiers to estimate demographic prevalence */
17         $\mathcal{D}_3^{\ominus} \leftarrow \{\mathbf{x}_i \in \mathcal{D}_3 \mid h(\mathbf{x}_i) = \ominus\}$  ;
18         $\mathcal{D}_3^{\oplus} \leftarrow \{\mathbf{x}_i \in \mathcal{D}_3 \mid h(\mathbf{x}_i) = \oplus\}$  ;
19         $\hat{p}_{\mathcal{D}_3^{\ominus}}^{q_{\ominus}}(s) \leftarrow q_{\ominus}(\mathcal{D}_3^{\ominus})$  ;
20         $\hat{p}_{\mathcal{D}_3^{\oplus}}^{q_{\oplus}}(s) \leftarrow q_{\oplus}(\mathcal{D}_3^{\oplus})$  ;
21        /* Compute the signed error of the demographic disparity
           estimate */
22         $e = \left[ \hat{p}_{\mathcal{D}_3^{\ominus}}^{q_{\ominus}}(s) - \hat{p}_{\mathcal{D}_3^{\oplus}}^{q_{\oplus}}(s) \right] - \left[ p_{\mathcal{D}_3^{\ominus}}(s) - p_{\mathcal{D}_3^{\oplus}}(s) \right]$  ;
23         $E \leftarrow E \cup \{e\}$ 
24      end
25    end
26  end
27 end
28  $\text{mae} \leftarrow \text{MAE}(E)$  ;
29  $\text{mse} \leftarrow \text{MSE}(E)$  ;
30 return mae, mse

```

Pseudocode 2: Protocol sample-size- \mathcal{D}_2 .

from $\check{\mathcal{D}}_2$. On the other hand, both SLD and HDy are fairly reliable. Once again, we find PCC to be the best performer, for the same reasons discussed in Section 5.3 and 5.4, i.e., the absence of shift between \mathcal{D}_2 and \mathcal{D}_3 . This sort of shift is actually a key variable for the estimation problem at hand and will be the target of the next experimental protocols, described in Sections 5.6 and 5.7.

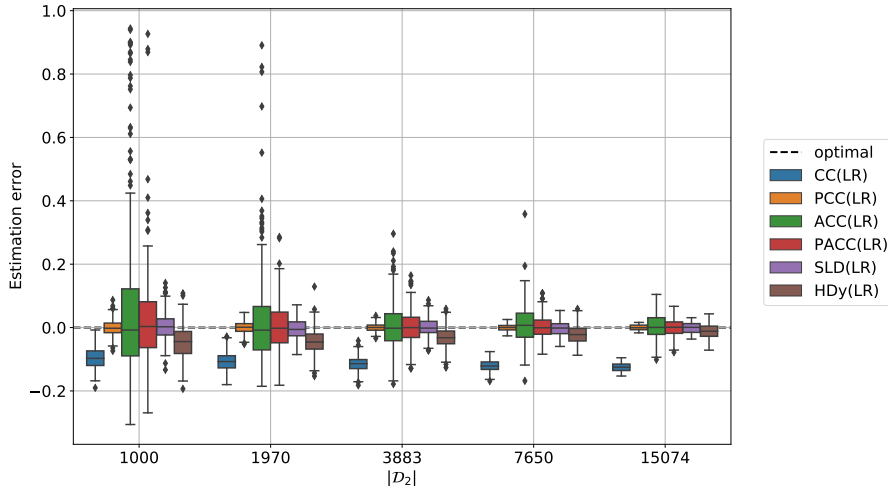


Fig. 3: Protocol **sample-size- \mathcal{D}_2** on the Adult dataset. Distribution of the estimation error (y axis) as the cardinality $|\mathcal{D}_2|$ is varied (x axis).

Table 6: Protocol **sample-size- \mathcal{D}_2**

		MAE	MSE	$P(\text{AE} < 0.1)$	$P(\text{AE} < 0.2)$
Adult	CC(LR)	0.113 \pm 0.026	0.013 \pm 0.005	0.259	1.000
	PCC(LR)	0.012 \pm 0.010	0.000 \pm 0.000	1.000	1.000
	ACC(LR)	0.077 \pm 0.114	0.019 \pm 0.085	0.797	0.941
	PACC(LR)	0.048 \pm 0.062	0.006 \pm 0.037	0.880	0.983
	SLD(LR)	0.023 \pm 0.019	0.001 \pm 0.002	0.995	1.000
	HDy(LR)	0.038 \pm 0.030	0.002 \pm 0.004	0.949	1.000
COMPAS	CC(LR)	0.213 \pm 0.058	0.049 \pm 0.027	0.016	0.447
	PCC(LR)	0.028 \pm 0.019	0.001 \pm 0.001	0.999	1.000
	ACC(LR)	0.299 \pm 0.213	0.135 \pm 0.177	0.185	0.383
	PACC(LR)	0.230 \pm 0.188	0.088 \pm 0.143	0.289	0.533
	SLD(LR)	0.122 \pm 0.091	0.023 \pm 0.032	0.488	0.807
	HDy(LR)	0.095 \pm 0.073	0.014 \pm 0.020	0.595	0.910
CreditCard	CC(LR)	0.105 \pm 0.056	0.014 \pm 0.014	0.476	0.943
	PCC(LR)	0.020 \pm 0.017	0.001 \pm 0.001	0.998	1.000
	ACC(LR)	0.321 \pm 0.254	0.168 \pm 0.237	0.224	0.389
	PACC(LR)	0.307 \pm 0.248	0.156 \pm 0.222	0.245	0.429
	SLD(LR)	0.064 \pm 0.054	0.007 \pm 0.012	0.813	0.971
	HDy(LR)	0.068 \pm 0.051	0.007 \pm 0.010	0.765	0.983

5.6 Protocol **sample-prev- \mathcal{D}_2**

5.6.1 Motivation and setup

The auxiliary set \mathcal{D}_2 can also display significant dataset shifts with respect to the the sets \mathcal{D}_1 and \mathcal{D}_3 available during training or at deployment. With this

experimental protocol, we assess the estimation error under shifts which affect either \mathcal{D}_2^\ominus or \mathcal{D}_2^\oplus , i.e., the subsets of \mathcal{D}_2 labelled positively or negatively by classifier h . We consider two experimental sub-protocols, describing variations in the prevalence of sensitive variable S in either subset. More specifically, we let $\Pr(s|\ominus)$ (or its dual $\Pr(s|\oplus)$) take 9 evenly spaced values between 0.1 and 0.9. We avoid extreme values of 0 and 1 which would make either demographic group $S = 0$ or $S = 1$ absent from the training set of one quantifier. To exemplify, in sub-protocol **sample-prev- \mathcal{D}_2^\ominus** we let the prevalence $\Pr(s|\ominus)$ in $\check{\mathcal{D}}_2^\ominus$ take values in $\{0.1, 0.2 \dots, 0.8, 0.9\}$, while the remaining subset $\check{\mathcal{D}}_2^\oplus$ remains at its natural prevalence $\Pr(s|\oplus)$.¹² For each repetition, we set $|\check{\mathcal{D}}_2^\ominus| = |\check{\mathcal{D}}_2^\oplus| = 500$. This makes for a challenging quantification setting and allows for fast training of multiple quantifiers across many repetitions. Pseudocode 3 describes the protocol when acting on \mathcal{D}_2^\ominus ; the case for \mathcal{D}_2^\oplus is analogous, and comes down to swapping the roles of \mathcal{D}_2^\ominus and \mathcal{D}_2^\oplus in Lines 12 and 13.

This protocol captures issues of representativeness in demographic data, e.g., due to non-uniform response rates across subpopulations (Schouten et al., 2009, 2012). Given the importance of trust for the provision of one’s sensitive attributes, in some domains this practice is considered akin to a *data donation* (Andrus et al., 2021). Individuals from groups that historically had worse quality or lower acceptance rates for a service can be hesitant to disclose their membership to said group, fearing it may be used against them as grounds for rejection or discrimination (Hasnain-Wynia and Baker, 2006). This may be especially true for individuals who perceive to be at high risk of rejection, bringing about complex selection biases, jointly dependent on S and Y , or S and \hat{Y} if individuals have some knowledge of the classification procedure. For example, health care providers are advised to collect information about patients’ race to monitor the quality of services across subpopulations. In a field study, 28% of patients reported discomfort about disclosure of their own race to a clerk, with black patients significantly less comfortable than white patients on average (Baker et al., 2005).

This is the first protocol we describe where quantifiers are trained on subsets $\check{\mathcal{D}}_2^\ominus, \check{\mathcal{D}}_2^\oplus$ that have a different prevalence for the sensitive variable S with respect to their counterparts $\mathcal{D}_3^\ominus, \mathcal{D}_3^\oplus$ in the deployment set. More specifically, with this protocol, we vary the joint distribution of (S, \hat{Y}) to directly influence the demographic disparity of the classifier h on the auxiliary set \mathcal{D}_2 , and move it away from the value $\Delta(s)$ of the same measure computed on the deployment set \mathcal{D}_3 . This is a fundamental evaluation protocol as it makes our estimand different across \mathcal{D}_2 (or, more precisely, its modified version $\check{\mathcal{D}}_2$) and \mathcal{D}_3 , which is typically expected in practice. If this were not the case, a practitioner could simply resort to an explicit computation of demographic disparity on the auxiliary set \mathcal{D}_2 and deem it representative of any deployment condition. Given this reasoning, we borrow this protocol from the quantification literature to cause sizeable variations in the demographic disparity of h across \mathcal{D}_2 and \mathcal{D}_3 , which act as the training and test set to different quantifiers. We expect these

¹² The natural prevalence is matched allowing for small fluctuations due to subsampling.


```

Input : • Dataset  $\mathcal{D}$  ;
          • Classifier learner CLS;
          • Quantification method Q;
Output: • MAE of the demographic disparity estimates ;
          • MSE of the demographic disparity estimates ;

1  $E \leftarrow \emptyset$  ;
2 for 5 random splits do
3    $\mathcal{D}_A, \mathcal{D}_B, \mathcal{D}_C \leftarrow \text{split\_stratify}(\mathcal{D})$  ;
4   for  $\mathcal{D}_1, \mathcal{D}_2, \mathcal{D}_3 \in \text{permutations}(\mathcal{D}_A, \mathcal{D}_B, \mathcal{D}_C)$  do
5     /* Learn a classifier  $h: X \rightarrow Y$  */
6      $h \leftarrow \text{CLS.fit}(\mathcal{D}_1)$  ;
7      $\mathcal{D}_2^\ominus \leftarrow \{(\mathbf{x}_i, s_i) \in \mathcal{D}_2 \mid h(\mathbf{x}_i) = \ominus\}$  ;
8      $\mathcal{D}_2^\oplus \leftarrow \{(\mathbf{x}_i, s_i) \in \mathcal{D}_2 \mid h(\mathbf{x}_i) = \oplus\}$  ;
9     for 10 repeats do
10      for  $p \in \{0.1, 0.2, \dots, 0.9\}$  do
11        /* Generate samples from  $\mathcal{D}_2^\ominus$  at desired prevalence and
12           size, and uniform samples from  $\mathcal{D}_2^\oplus$  at desired size */
13         $\check{\mathcal{D}}_2^\ominus \sim \mathcal{D}_2^\ominus$  with  $p_{\check{\mathcal{D}}_2^\ominus}(s) = p$  and  $|\check{\mathcal{D}}_2^\ominus| = 500$  ;
14         $\check{\mathcal{D}}_2^\oplus \sim \mathcal{D}_2^\oplus$  with  $|\check{\mathcal{D}}_2^\oplus| = 500$  ;
15        /* Learn quantifiers  $q_y: 2^{\mathcal{X}} \rightarrow [0, 1]$  */
16         $q_\ominus \leftarrow \text{Q.fit}(\check{\mathcal{D}}_2^\ominus)$  ;
17         $q_\oplus \leftarrow \text{Q.fit}(\check{\mathcal{D}}_2^\oplus)$  ;
18        /* Use quantifiers to estimate demographic prevalence */
19         $\mathcal{D}_3^\ominus \leftarrow \{\mathbf{x}_i \in \mathcal{D}_3 \mid h(\mathbf{x}_i) = \ominus\}$  ;
20         $\mathcal{D}_3^\oplus \leftarrow \{\mathbf{x}_i \in \mathcal{D}_3 \mid h(\mathbf{x}_i) = \oplus\}$  ;
21         $\hat{p}_{\mathcal{D}_3^\ominus}^{q_\ominus}(s) \leftarrow q_\ominus(\mathcal{D}_3^\ominus)$  ;
22         $\hat{p}_{\mathcal{D}_3^\oplus}^{q_\oplus}(s) \leftarrow q_\oplus(\mathcal{D}_3^\oplus)$  ;
23        /* Compute the signed error of the demographic disparity
24           estimate */
25         $e = \left[ \hat{p}_{\mathcal{D}_3^\ominus}^{q_\ominus}(s) - \hat{p}_{\mathcal{D}_3^\oplus}^{q_\oplus}(s) \right] - \left[ p_{\mathcal{D}_3^\ominus}(s) - p_{\mathcal{D}_3^\oplus}(s) \right]$  ;
26         $E \leftarrow E \cup \{e\}$ 
27      end
28    end
29  end
30   $\text{mae} \leftarrow \text{MAE}(E)$  ;
31   $\text{mse} \leftarrow \text{MSE}(E)$  ;
32  return mae, mse

```

Pseudocode 3: Protocol $\text{sample-prev-}\mathcal{D}_2$, shown for variations of prevalence values in class $y = \ominus$.

variations to bring about clear trends in the estimation error of demographic parity for the approaches considered in this work.

5.6.2 Results

Figure 4 depicts the estimation error on the y axis, as we vary, on the x axis, the sensitive attribute prevalence in \mathcal{D}_2^\ominus (Figure 4a) and \mathcal{D}_2^\oplus (Figure 4b). CC,

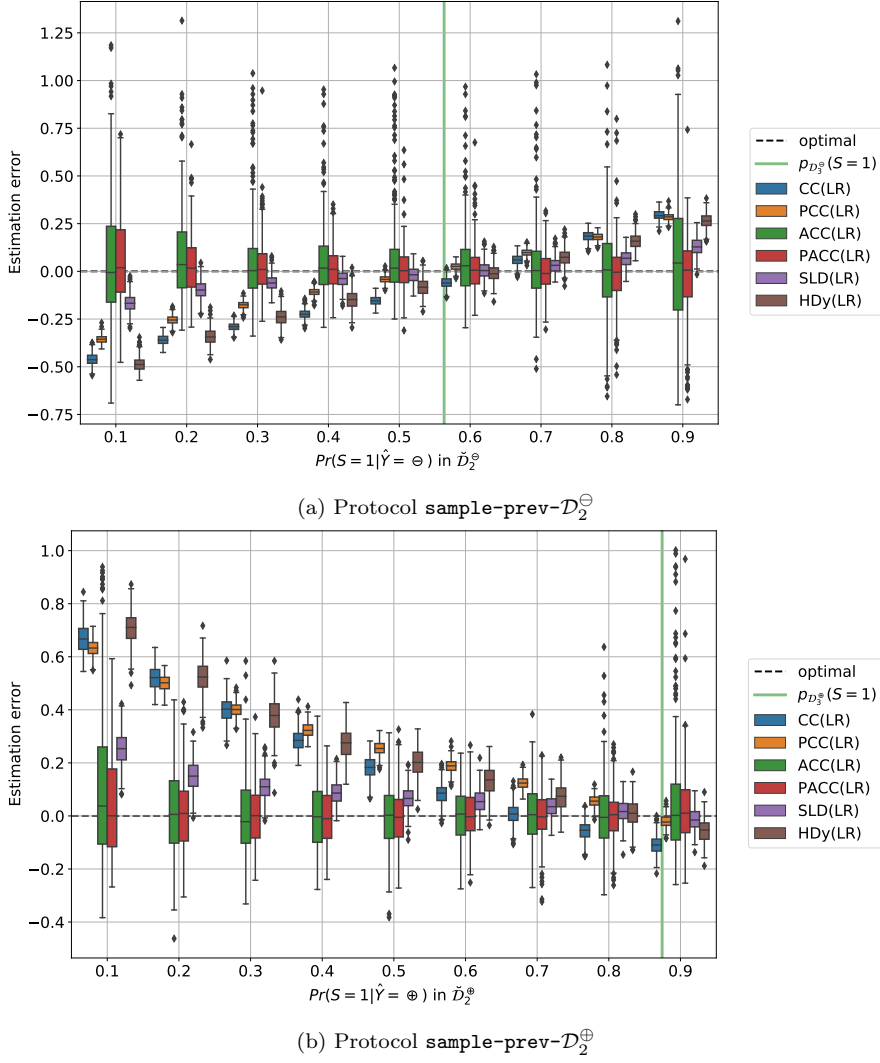


Fig. 4: Protocol **sample-prev- \mathcal{D}_2** on the Adult dataset. Distribution of the estimation error (y axis) as $\tilde{\mathcal{D}}_2$ is sampled with a given $\Pr(S = 1|Y = \ominus)$ value, plot (a), or $\Pr(S = 1|Y = \oplus)$ value, plot (b) (x axis). The green line indicates the value of $\Pr(S = 1)$ as observed in \mathcal{D}_3^\ominus , plot (a), or \mathcal{D}_3^\oplus , plot (b).

PCC, and HDy stand out as fairly sensitive to shifts in their training set. In sub-protocol **sample-prev- \mathcal{D}_2^\oplus** , summarized in Figure 4b, we have that the prevalence of males in the subset \mathcal{D}_2^\oplus , used to train one of the quantifiers, is almost always lower than the prevalence in the respective test subset \mathcal{D}_3^\oplus ,

Table 7: Protocol **sample-prev- \mathcal{D}_2** .

		MAE	MSE	$P(\text{AE} < 0.1)$	$P(\text{AE} < 0.2)$
Adult	CC(LR)	0.246 \pm 0.179	0.093 \pm 0.118	0.266	0.472
	PCC(LR)	0.224 \pm 0.167	0.078 \pm 0.103	0.277	0.523
	ACC(LR)	0.148 \pm 0.157	0.047 \pm 0.122	0.474	0.775
	PACC(LR)	0.104 \pm 0.095	0.020 \pm 0.045	0.590	0.884
	SLD(LR)	0.085 \pm 0.069	0.012 \pm 0.019	0.670	0.924
	HDy(LR)	0.235 \pm 0.190	0.091 \pm 0.132	0.298	0.519
COMPAS	CC(LR)	0.421 \pm 0.265	0.248 \pm 0.240	0.079	0.262
	PCC(LR)	0.246 \pm 0.167	0.089 \pm 0.103	0.233	0.463
	ACC(LR)	0.390 \pm 0.275	0.228 \pm 0.281	0.143	0.285
	PACC(LR)	0.277 \pm 0.222	0.126 \pm 0.197	0.229	0.451
	SLD(LR)	0.147 \pm 0.118	0.036 \pm 0.057	0.425	0.726
	HDy(LR)	0.237 \pm 0.174	0.086 \pm 0.112	0.259	0.490
CreditCard	CC(LR)	0.386 \pm 0.258	0.216 \pm 0.222	0.128	0.317
	PCC(LR)	0.229 \pm 0.144	0.073 \pm 0.076	0.231	0.460
	ACC(LR)	0.433 \pm 0.315	0.287 \pm 0.326	0.189	0.297
	PACC(LR)	0.428 \pm 0.310	0.279 \pm 0.320	0.187	0.296
	SLD(LR)	0.197 \pm 0.135	0.057 \pm 0.068	0.289	0.555
	HDy(LR)	0.244 \pm 0.157	0.084 \pm 0.091	0.219	0.439

reported with a vertical green line.¹³ As a result, quantifiers trained on \mathcal{D}_2^\oplus tend to systematically underestimate the prevalence of males in \mathcal{D}_3^\oplus and overestimate the (signed) demographic disparity of classifier h as a result. Similar considerations hold for sub-protocol **sample-prev- \mathcal{D}_2^\ominus** , with a sign flip due to $p_{\mathcal{D}_3^\ominus}(s)$ being the first term in Equation 10. Although less substantial, also SLD displays similar trends.

The remaining methods, ACC and PACC, have a good median performance, compensating this type of shift with the respective adjustments. On the negative side, they display a large variance, due to a small cardinality of the auxiliary set in this protocol, which makes adjustments particularly unstable, as seen under protocol **sample-size- \mathcal{D}_2** (Section 5.5). These effects are particularly evident at the extrema of the x axis, which correspond to settings where few instances with either $S = 0$ or $S = 1$ are available for quantifier training. In turn, the few positives (negatives) make it particularly difficult to estimate the tpr (tnr) of k reliably, as required by Equations (5) and (7). For example, in Figure 4a we see ACC reaching error rates that range between -0.7 and 1.3 . Given that the true demographic disparity of the classifier h is $\Delta(s) = -0.3$, these are the worst possible errors, corresponding to extreme estimates $\hat{\Delta}(s) = -1$ and $\hat{\Delta}(s) = 1$, respectively.

Similar trends also hold for COMPAS and CreditCard as summarized in Table 7. Overall, SLD seems to strike the best balance between bias and variance. It is worth noting that (1) with this protocol we tested extreme shifts in the prevalence of sensitive attribute between the auxiliary set \mathcal{D}_2 and de-

¹³ This is true for every data point on the x axis in Figure 4b, except for the rightmost one, where $p_{\mathcal{D}_2^\oplus}(s) = 0.9 > p_{\mathcal{D}_3^\oplus}(s) = 0.85$.

ployment set \mathcal{D}_3 and that (2) the summary in Table 7 treats every prevalence as equally likely, while in practice we expect that extreme shifts will be less probable, helping to bound the estimation errors closer to zero. Indeed, in Figure 4 every method performs better in a proximity of the test prevalence.

5.7 Protocol **sample-prev- \mathcal{D}_3**

5.7.1 Motivation and setup

This is essentially the counterpart of protocol **sample-prev- \mathcal{D}_2** (Section 5.6), focusing on shifts in the test set \mathcal{D}_3 . Similarly, we consider two sub-protocols that model changes in the prevalence of a sensitive variable S in the test subset of either positively or negatively predicted instances, called \mathcal{D}_3^\ominus and \mathcal{D}_3^\oplus . More in detail, we let $\Pr(s|\ominus)$ (or its dual $\Pr(s|\oplus)$) in $\check{\mathcal{D}}_3$ take eleven evenly spaced values between 0 and 1. For example, under sub-protocol **sample-prev- \mathcal{D}_3^\ominus** , we vary the prevalence of sensitive attribute S in $\check{\mathcal{D}}_3^\ominus$, so that $\Pr(s|\ominus) \in \{0.0, 0.1, \dots, 0.9, 1.0\}$, while keeping the prevalence in $\check{\mathcal{D}}_3^\oplus$ fixed. Contrary to protocol **sample-prev- \mathcal{D}_2** , here we also allow for extreme prevalence values of 0 and 1 for the sensitive attribute S , as this does not invalidate the quantifiers' training. For both sub-protocols, in each repetition we sample subsets of the test set \mathcal{D}_3 such that $|\check{\mathcal{D}}_3^\ominus| = |\check{\mathcal{D}}_3^\oplus| = 500$. Pseudocode 4 describes the protocol when acting on \mathcal{D}_3^\ominus ; the case for \mathcal{D}_3^\oplus is analogous, and comes down to swapping the roles of \mathcal{D}_3^\ominus and \mathcal{D}_3^\oplus in Lines 18 and 19. Note that the pale red region (delimiting the protocol-specific computations) comprises the computation of the error (line 24) since, in this case, the error is computed with respect to the samples $\check{\mathcal{D}}_3^\ominus$ and $\check{\mathcal{D}}_3^\oplus$, and not with respect to \mathcal{D}_3^\ominus and \mathcal{D}_3^\oplus .

This protocol accounts for the inevitable evolution of phenomena, especially those related to human behaviour. Indeed, it is common in real-world scenarios for data generation processes to be non-stationary and change across training and test, due e.g., to seasonality or any sort of unmodelled novelty and difference in populations (Ditzler et al., 2015; Malinin et al., 2021; Moreno-Torres et al., 2012). Given most work on algorithmic fairness focuses on decisions or predictions about people, and given the unavoidable role of change in human lives, values, and behaviour, the above considerations about non-stationarity seem particularly relevant in this context. For instance, data available from one population is often repurposed to train algorithms that will be deployed on a different population, requiring ad-hoc fair learning approaches (Coston et al., 2019) and evoking the *portability trap* of fair machine learning (Selbst et al., 2019). Moreover, agents may be responsive to novel technology in their social context and adapt their behaviour accordingly (Hu et al., 2019; Tsirtsis et al., 2019), causing *ripple effects* (Selbst et al., 2019) and *feedback loops* (Mansoury et al., 2020). Furthermore, as a concrete (although spurious) example of a shift in a popular fairness dataset, the repeated offense rate for black and white defendants in the COMPAS dataset (Larson et al., 2016) increases sharply between 2013 and 2014 (Barenstein, 2019; Biswas and Mukher-

jee, 2021). As a final example, personalized pricing constitutes an increasingly possible practice with non-trivial fairness concerns (Kallus and Zhou, 2021) and inevitable shifts due to changing habits and environments (Sindreu, 2021).

In the quantification literature, this is the most common evaluation protocol. Similarly to **sample-prev- \mathcal{D}_2** , it imposes shifts in the estimand between the training and testing conditions of a quantifier, represented by the auxiliary set \mathcal{D}_2 and the deployment set \mathcal{D}_3 , respectively. Through this protocol, we expect to find similar patterns to those highlighted in Section 5.6, with the roles of the auxiliary set \mathcal{D}_2 and test set \mathcal{D}_3 now switched. Under this protocol, \mathcal{D}_3 has a smaller cardinality and variable prevalence (and is referred to as $\check{\mathcal{D}}_3$ for this reason), while \mathcal{D}_2 is left to its original cardinality and prevalence of sensitive attribute S .

5.7.2 Results

The estimation error under this protocol is reported in Figure 5, on the y axis, as we vary the prevalence of protected groups in the test set, on the x axis. Figure 5a concentrates on prevalence variations in \mathcal{D}_3^\ominus , while Figure 5b considers variations of the prevalence of protected groups in \mathcal{D}_3^\oplus . Similar trends emerge under both sub-protocols. Similarly to Section 5.6, both CC and PCC display a clear trend along the x axis, vastly over- or under-estimating the demographic disparity of h , and proving to be rather unreliable in settings where the priors of their test set drift away from the priors of their training set. In sub-protocol **sample-prev- \mathcal{D}_3^\oplus** , symmetrically to sub-protocol **sample-prev- \mathcal{D}_2^\oplus** , we have that the prevalence of males in the subset $\check{\mathcal{D}}_3^\oplus$, used to test one of the quantifiers, is almost always lower than the prevalence in the respective training subset \mathcal{D}_2^\oplus . As a result, CC tends to systematically overestimate the prevalence of males in $\check{\mathcal{D}}_3^\oplus$ and underestimate the (signed) demographic disparity of classifier h as a result.

ACC, PACC, and HDy are three methods that require splitting the training set to estimate auxiliary quantities. With respect to protocol **sample-prev- \mathcal{D}_2** , where $|\check{\mathcal{D}}_2|=1,000$, in this experiment they all benefit from a larger training set, reducing the bias of HDy and the variance of ACC and PACC. Finally, SLD maintains a reliable performance. Analogous results obtain on COMPAS and CreditCard, as summarized in Table 8. Similarly to Table 7, we find that, under large shifts between the auxiliary and deployment set, the estimation of demographic disparity is more difficult on COMPAS and CreditCard than on the Adult dataset.

5.8 Ablation study

5.8.1 Motivation and setup

In Sections 5.3–5.7 we tested six approaches to estimate demographic disparity. For each approach, we exploited multiple quantifiers for the sensitive attribute

```

Input : • Dataset  $\mathcal{D}$  ;
          • Classifier learner CLS;
          • Quantification method Q;
Output: • MAE of the demographic disparity estimates ;
          • MSE of the demographic disparity estimates ;

1  $E \leftarrow \emptyset$  ;
2 for 5 random splits do
3    $\mathcal{D}_A, \mathcal{D}_B, \mathcal{D}_C \leftarrow \text{split\_stratify}(\mathcal{D})$  ;
4   for  $\mathcal{D}_1, \mathcal{D}_2, \mathcal{D}_3 \in \text{permutations}(\mathcal{D}_A, \mathcal{D}_B, \mathcal{D}_C)$  do
5     /* Learn a classifier  $h: X \rightarrow Y$  */
6      $h \leftarrow \text{CLS.fit}(\mathcal{D}_1)$  ;
7      $\mathcal{D}_2^\ominus \leftarrow \{(\mathbf{x}_i, s_i) \in \mathcal{D}_2 \mid h(\mathbf{x}_i) = \ominus\}$  ;
8      $\mathcal{D}_2^\oplus \leftarrow \{(\mathbf{x}_i, s_i) \in \mathcal{D}_2 \mid h(\mathbf{x}_i) = \oplus\}$  ;
9     /* Learn quantifiers  $q_y: 2^{\mathcal{X}} \rightarrow [0, 1]$  */
10     $q_\ominus \leftarrow \text{Q.fit}(\mathcal{D}_2^\ominus)$  ;
11     $q_\oplus \leftarrow \text{Q.fit}(\mathcal{D}_2^\oplus)$  ;
12    /* Split instances in  $\mathcal{D}_3$  based on predicted labels from  $h$  */
13     $\mathcal{D}_3^\ominus \leftarrow \{\mathbf{x}_i \in \mathcal{D}_3 \mid h(\mathbf{x}_i) = \ominus\}$  ;
14     $\mathcal{D}_3^\oplus \leftarrow \{\mathbf{x}_i \in \mathcal{D}_3 \mid h(\mathbf{x}_i) = \oplus\}$  ;
15    for 10 repeats do
16      for  $p \in \{0.1, 0.2, \dots, 0.9\}$  do
17        /* Generate samples from  $\mathcal{D}_3^\ominus$  at desired prevalence and
18           size, and uniform samples from  $\mathcal{D}_3^\oplus$  at desired size */
19         $\check{\mathcal{D}}_3^\ominus \sim \mathcal{D}_3^\ominus$  with  $p_{\check{\mathcal{D}}_3^\ominus}(s) = p$  and  $|\check{\mathcal{D}}_3^\ominus| = 500$  ;
20         $\check{\mathcal{D}}_3^\oplus \sim \mathcal{D}_3^\oplus$  with  $|\check{\mathcal{D}}_3^\oplus| = 500$  ;
21        /* Use quantifiers to estimate demographic prevalence */
22         $\hat{p}_{\check{\mathcal{D}}_3^\ominus}^{q_\ominus}(s) \leftarrow q_\ominus(\check{\mathcal{D}}_3^\ominus)$  ;
23         $\hat{p}_{\check{\mathcal{D}}_3^\oplus}^{q_\oplus}(s) \leftarrow q_\oplus(\check{\mathcal{D}}_3^\oplus)$  ;
24        /* Compute the signed error of the demographic disparity
25           estimate */
26         $e = \left[ \hat{p}_{\check{\mathcal{D}}_3^\ominus}^{q_\ominus}(s) - \hat{p}_{\check{\mathcal{D}}_3^\oplus}^{q_\oplus}(s) \right] - \left[ p_{\check{\mathcal{D}}_3^\ominus}(s) - p_{\check{\mathcal{D}}_3^\oplus}(s) \right]$  ;
27         $E \leftarrow E \cup \{e\}$ 
28      end
29    end
30  end
31   $\text{mae} \leftarrow \text{MAE}(E)$  ;
32   $\text{mse} \leftarrow \text{MSE}(E)$  ;
33 return mae, mse

```

Pseudocode 4: Protocol `sample-prev- \mathcal{D}_3` , shown for variations of prevalence values in class $y = \ominus$.

S , namely one for each class in the codomain of classifier h . In the binary setting adopted in this work, where $\mathcal{Y} = \{\ominus, \oplus\}$, we trained two quantifiers. One quantifier was trained on the set of positively-classified instances of the auxiliary set $\mathcal{D}_2^\oplus = \{(\mathbf{x}_i, s_i) \in \mathcal{D}_2 \mid h(\mathbf{x}) = \oplus\}$ and deployed to quantify the prevalence of sensitive instances (such that $S = s$) within the deployment subset \mathcal{D}_3^\oplus . The remaining quantifier was trained on \mathcal{D}_2^\ominus and deployed on \mathcal{D}_3^\ominus .

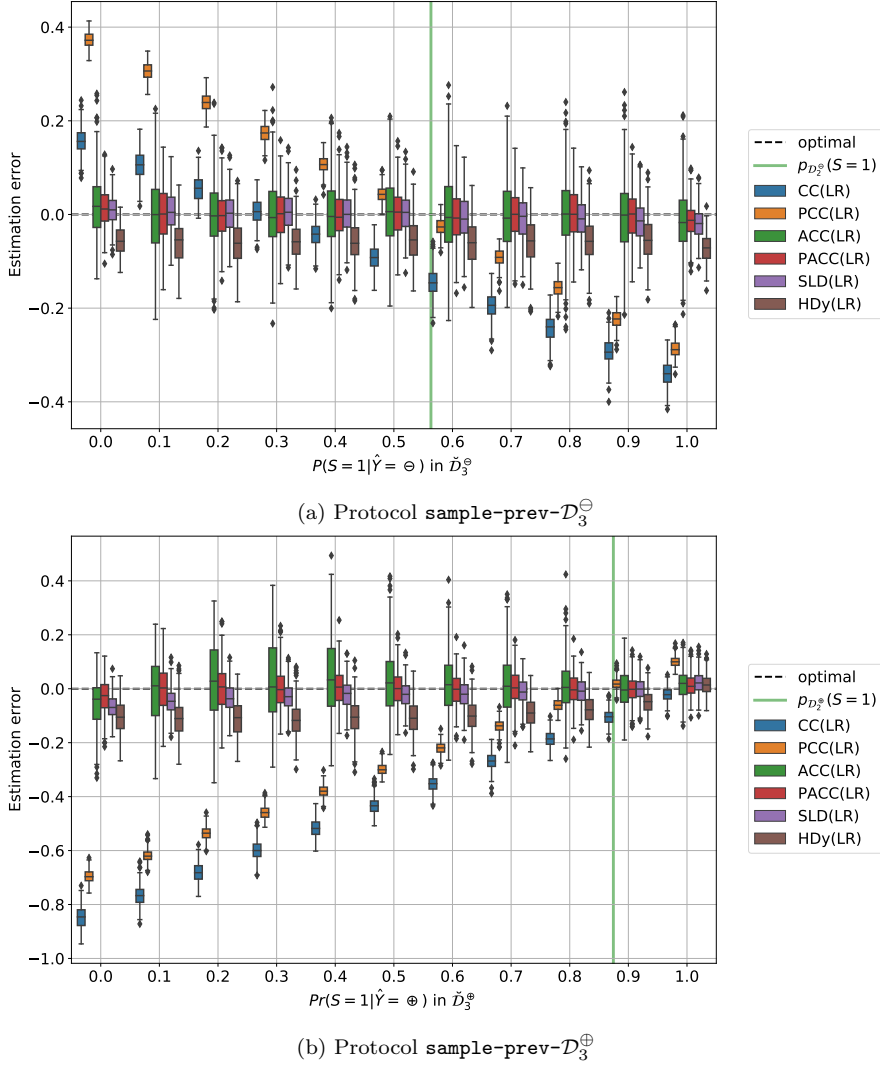


Fig. 5: Protocol **sample-prev- \mathcal{D}_3** on the Adult dataset. Distribution of the estimation error (y axis) as $\tilde{\mathcal{D}}_3$ is sampled with a given $Pr(S=1|Y=\ominus)$ value, plot (a), or $Pr(S=1|Y=\oplus)$ value, plot (b) (x axis). The green line indicates the value of $Pr(S=1)$ as observed in \mathcal{D}_2^\ominus , plot (a), or \mathcal{D}_2^\oplus , plot (b).

Training and maintaining multiple quantifiers is more expensive and cumbersome than having a single one. Firstly, quantifiers that depend on the classification outcome $\hat{y} = h(\mathbf{x})$ require re-training every time h is modified, e.g., due to a model update being rolled out. Secondly, the cost of maintenance is multiplied by the number of classes $|\mathcal{Y}|$ that are possible for the outcome variable. To ensure these downsides are compensated by performance improve-

Table 8: Protocol **sample-prev- \mathcal{D}_3** .

		MAE	MSE	$P(\text{AE} < 0.1)$	$P(\text{AE} < 0.2)$
Adult	CC(LR)	0.294 \pm 0.244	0.146 \pm 0.204	0.251	0.467
	PCC(LR)	0.253 \pm 0.189	0.099 \pm 0.130	0.252	0.464
	ACC(LR)	0.077 \pm 0.064	0.010 \pm 0.017	0.720	0.947
	PACC(LR)	0.047 \pm 0.037	0.004 \pm 0.005	0.909	0.997
	SLD(LR)	0.040 \pm 0.031	0.003 \pm 0.004	0.947	1.000
	HDy(LR)	0.078 \pm 0.052	0.009 \pm 0.011	0.694	0.975
COMPAS	CC(LR)	0.366 \pm 0.269	0.206 \pm 0.246	0.198	0.357
	PCC(LR)	0.287 \pm 0.188	0.118 \pm 0.131	0.189	0.379
	ACC(LR)	0.399 \pm 0.289	0.243 \pm 0.324	0.134	0.285
	PACC(LR)	0.199 \pm 0.180	0.072 \pm 0.137	0.351	0.627
	SLD(LR)	0.143 \pm 0.109	0.032 \pm 0.046	0.430	0.736
	HDy(LR)	0.217 \pm 0.165	0.074 \pm 0.109	0.278	0.536
CreditCard	CC(LR)	0.276 \pm 0.177	0.107 \pm 0.117	0.192	0.390
	PCC(LR)	0.276 \pm 0.168	0.104 \pm 0.103	0.187	0.374
	ACC(LR)	0.311 \pm 0.229	0.149 \pm 0.204	0.200	0.380
	PACC(LR)	0.230 \pm 0.176	0.084 \pm 0.120	0.276	0.516
	SLD(LR)	0.158 \pm 0.119	0.039 \pm 0.056	0.386	0.690
	HDy(LR)	0.205 \pm 0.155	0.066 \pm 0.092	0.302	0.569

ments, we perform an ablation study evaluating the performance of different estimators of demographic disparity supported by a single quantifier.

In this section, we concentrate on three estimation approaches, namely CC, SLD and PACC. CC is chosen as the naïve baseline adopted by practitioners unaware of ad-hoc approaches for prevalence estimation. SLD and PACC are among the best performers in Sections 5.3–5.7, displaying low bias or variance across all protocols. We compare their performance under two settings. In the first setting, adopted thus far, two separate quantifiers q_{\ominus} and q_{\oplus} are trained on \mathcal{D}_2^{\ominus} , \mathcal{D}_2^{\oplus} and deployed on \mathcal{D}_3^{\ominus} , \mathcal{D}_3^{\oplus} , respectively. In the second setting, we train a single quantifier q on \mathcal{D}_2 and deploy it separately on \mathcal{D}_3^{\ominus} and \mathcal{D}_3^{\oplus} to estimate $\hat{\Delta}(s)$ via Equation 12, specialized so that q_{\ominus} and q_{\oplus} are the same quantifier.

5.8.2 Results

Figure 6 summarizes results for the Adult dataset under two protocols that are representative of the overall trends, namely **flip-prev- \mathcal{D}_1** (Figure 6a) and **sample-size- \mathcal{D}_2** (Figure 6b).¹⁴ The y axis depicts the estimation error of CC, SLD, PACC, and their single-quantifier counterparts, denoted with suffix “nosD2” to indicate that the auxiliary set \mathcal{D}_2 is not split into \mathcal{D}_2^{\ominus} , \mathcal{D}_2^{\oplus} during training. The x axis depicts the quantity of interest varied under each protocol.

¹⁴ In the interest of brevity, the figures in this section refer to LR-based quantification on the Adult dataset under two protocols. Results for SVM-based quantifiers under every protocol are depicted in the Appendix (Figures 9 – 13). Analogous results hold on CreditCard and COMPAS.

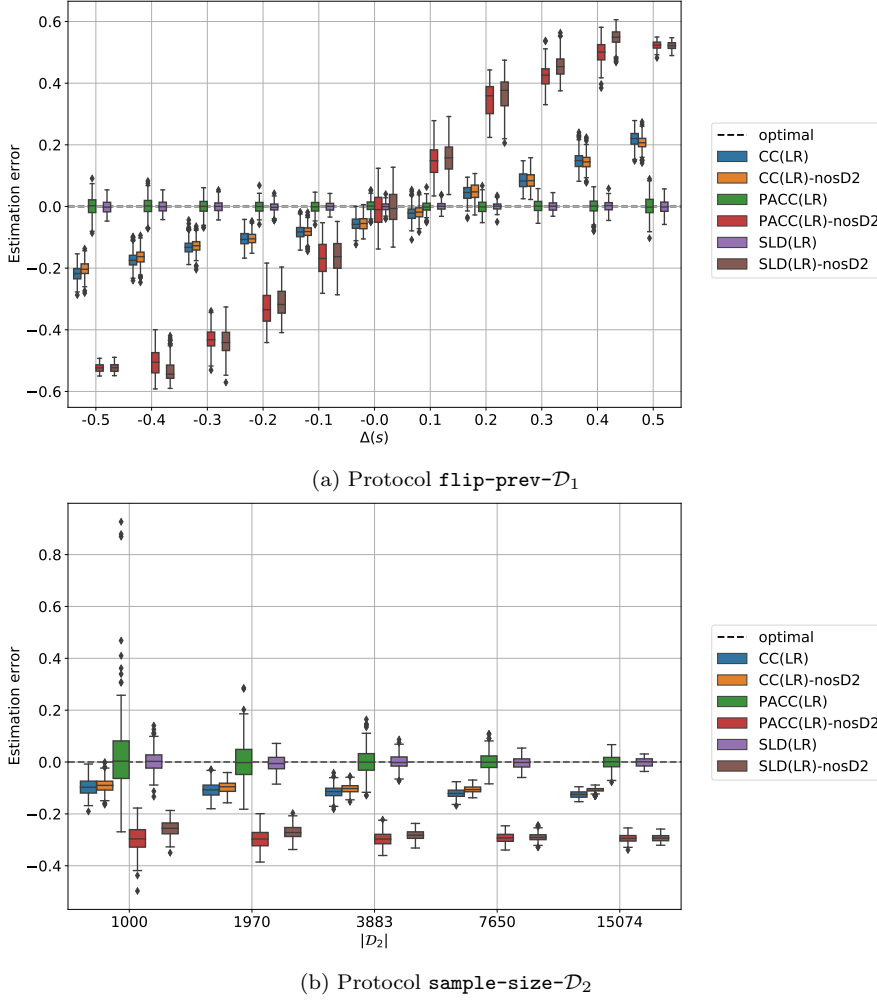


Fig. 6: Ablation study on the Adult dataset. Distribution of the estimation error (y axis) for CC, PACC, SLD, and their single-quantifier counterparts, as $\Delta(s)$, plot (a), and $|D_2|$, plot (b), are varied (x axis).

Interestingly, CC appears to be rather insensitive to the ablation study, so that the estimation errors of CC and CC-nosD2 are well-aligned (although they both fare poorly). The opposite is true for both PACC and SLD. These quantification approaches display a clear decay in performance in the single-quantifier setting. Under protocol **flip-prev- \mathcal{D}_1** (Figure 6a) both PACC-nosD2 and SLD-nosD2 have large estimation errors, which vary along the x axis, and are consistently worse than CC. On the other hand, under protocol **sample-size- \mathcal{D}_2** (Figure 6b) PACC-nosD2 and SLD-nosD2 display a more

moderate yet sizeable performance decay, which is mostly constant along the x axis.

Under all protocols, the performance of SLD and PACC is compromised in the absence of class-specific quantifiers q_{\ominus} and q_{\oplus} . If a single quantifier is trained on the full auxiliary set \mathcal{D}_2 , the corrections brought about by SLD and PACC end up worsening, rather than improving, the prevalence estimates of vanilla CC. For this reason, the ideal workflow requires partitioning the auxiliary set into subsets \mathcal{D}_2^{\ominus} and \mathcal{D}_2^{\oplus} , as illustrated in Section 4.

5.9 Quantifying without classifying

5.9.1 Motivation and setup

The motivating use case for this work are internal audits of group fairness, to characterize a model and its potential to harm sensitive categories of users. Following Awasthi et al. (2021), we envision this as an important first step to empower practitioners in arguing for resources and, more broadly, advocate for deeper understanding and careful evaluation of models. Unfortunately, developing a tool to infer demographic information, even if motivated by careful intentions and good faith, leaves open the possibility for misuse, especially at an individual level. Once a predictive tool, also capable of instance-level classification, is available, it will be tempting for some actors to exploit it precisely for this purpose.

For example, the *Bayesian Improved Surname Geocoding* (BISG) method (Elliott et al., 2009) is intended to estimate population-level disparities in health care. However, it was also used to identify individuals potentially eligible for settlements related to discriminatory practices by auto lending companies (Andriotis and Ensign, 2015; Koren, 2016). Automatic inference of sensitive attributes of individuals is problematic for several reasons. Such procedure exploits the co-occurrence of membership in a group and display of a given trait, running the risk of learning, encoding and reinforcing stereotypical associations. While also true of group-level estimates, this practice is particularly troublesome at an individual level, where it is likely to cause harms for people who do not fit the norm, resulting, for instance, in misgendering and the associated negative effects (McLemore, 2015). Even when “accurate”, the mere act of externally assigning sensitive labels can be problematic. For example, gender assignment may be forceful and lead to psychological harm for individuals (Keyes, 2018).

In this section, we aim to demonstrate that it is possible to decouple the objective of (group-level) quantification of sensitive attributes from that of (individual-level) classification. For protocols in previous sections, we compute the accuracy and F_1 score (defined below) of the sensitive attribute classifier k underlying the tested quantifiers, comparing it against their estimation error for class prevalence of the sensitive attribute S (Equation 13). Accuracy is the proportion of correctly classified instances over the total (Equation 16) while

F_1 is the harmonic mean of precision and recall (Equation 17). Both measures can be computed from the counters of true positives (TP), true negatives (TN), false positives (FP), and false negatives (FN), as follows:

$$\text{accuracy} = \frac{\text{TP} + \text{TN}}{\text{TP} + \text{TN} + \text{FP} + \text{FN}} \quad (16)$$

$$F_1 = \begin{cases} \frac{2\text{TP}}{2\text{TP} + \text{FP} + \text{FN}} & \text{if } \text{TP} + \text{FP} + \text{FN} > 0 \\ 1 & \text{if } \text{TP} = \text{FP} = \text{FN} = 0 \end{cases} \quad (17)$$

5.9.2 Results

Figures 7 and 8 displays the quantification performance (MAE) and classification performance (F_1 , accuracy) of CC, SLD and PACC on the Adult dataset under protocols **sample-prev- \mathcal{D}_2** and **sample-prev- \mathcal{D}_3** , respectively. As usual, we describe results for LR-based learners and report their SVM-based duals in the Appendix (Figures 14 and 15). To evaluate the quantification performance of each approach, we simply report their MAE in estimating the prevalence $p_{\mathcal{D}_3^\ominus}(S=1)$, $p_{\mathcal{D}_3^\oplus}(S=1)$ in either test subset, depending on the protocol at hand. To assess the performance of the sensitive attribute classifier k underlying each quantifier, we proceed as follows. For CC and PACC, we simply run k (LR) on either \mathcal{D}_3^\ominus or \mathcal{D}_3^\oplus , reporting its accuracy and F_1 score in inferring the sensitive attribute of individual instances. The classification performance of the classifiers underlying CC and PACC are equivalent, so we omit the latter from Figures 14 and 15 for readability. For SLD, we take the novel posteriors obtained by applying the EM algorithm to either test subset, and use them for classification with a threshold of 0.5.

Clearly, SLD improves both the quantification and classification performance of the classifier k . In terms of quantification, its MAE is consistently below that of CC, and in terms of classification it displays better F_1 and accuracy. However, under large prevalence shifts across the auxiliary set \mathcal{D}_2 and the test set \mathcal{D}_3 , its classification performance becomes unreliable. In particular, under protocol **sample-prev- \mathcal{D}_3^\ominus** (resp. **sample-prev- \mathcal{D}_3^\oplus**) in Figure 8a (resp. Figure 8b), for low values of the x axis, i.e., when the true prevalence values $p_{\mathcal{D}_3^\ominus}(S=1)$ (resp. $p_{\mathcal{D}_3^\oplus}(S=1)$) becomes small, the SLD-based classifier starts acting as a trivial rejector with low recall, hence low F_1 score. On the other hand, the quantification performance of SLD does not degrade in the same way, as its MAE is low and flat across the entire x axis in Figures 8a and 8b. This is a first hint to the fact that classification and quantification performance may be decoupled.

PACC is another method which significantly outperforms CC in estimating the prevalence of sensitive attributes in both test subsets \mathcal{D}_3^\ominus , \mathcal{D}_3^\oplus . Indeed, its MAE is well-aligned with that of SLD, displaying low quantification error under every protocol (Figures 7–8). On the other hand, its classification

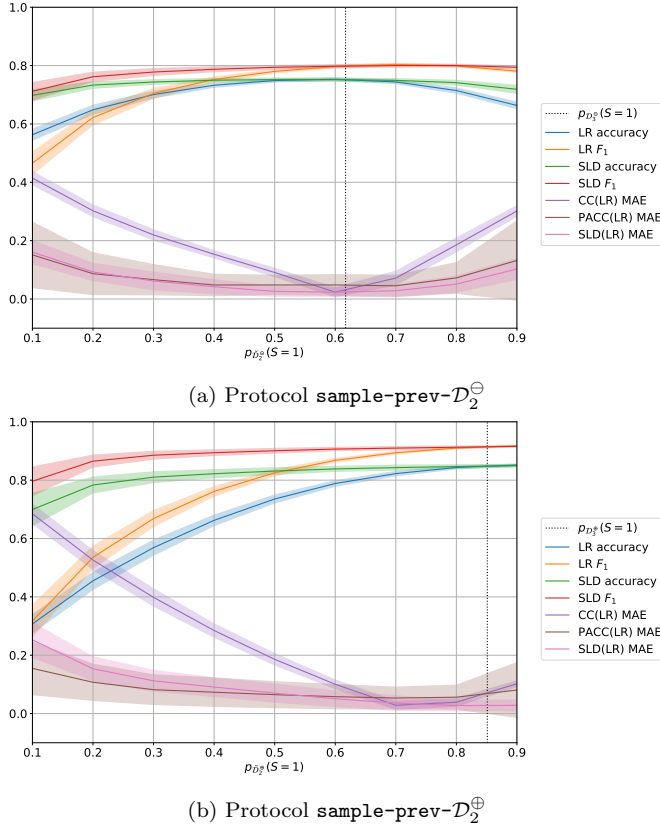


Fig. 7: Performance of CC, SLD and PACC on the Adult dataset when used for quantification (MAE – lower is better) and classification (F_1 , accuracy – higher is better) under protocol **sample-prev- \mathcal{D}_2** . The classification performance of PACC is equivalent to that of CC (both equal to the performance of the underlying LR), and we thus omit it for readability.

performance is aligned with the accuracy and F_1 score of CC, which is unsatisfactory and can even become worse than random. This fact shows that it is possible to build models which yield good prevalence estimates for the sensitive attribute within a sample, without providing reliable demographic estimates for single instances. Indeed, quantification methods of type *aggregative* (i.e., based on the outcomes of a classifier – like all methods we use in this study) are suited to repair the initial prevalence estimate (computed by classifying and counting) without precise knowledge of which specific data items have been misclassified. In the context of models to measure fairness under unawareness of sensitive attributes, we highlight this as a positive result, decoupling a desirable ability to estimate group-level disparities from an undesirable misuse at the individual level.

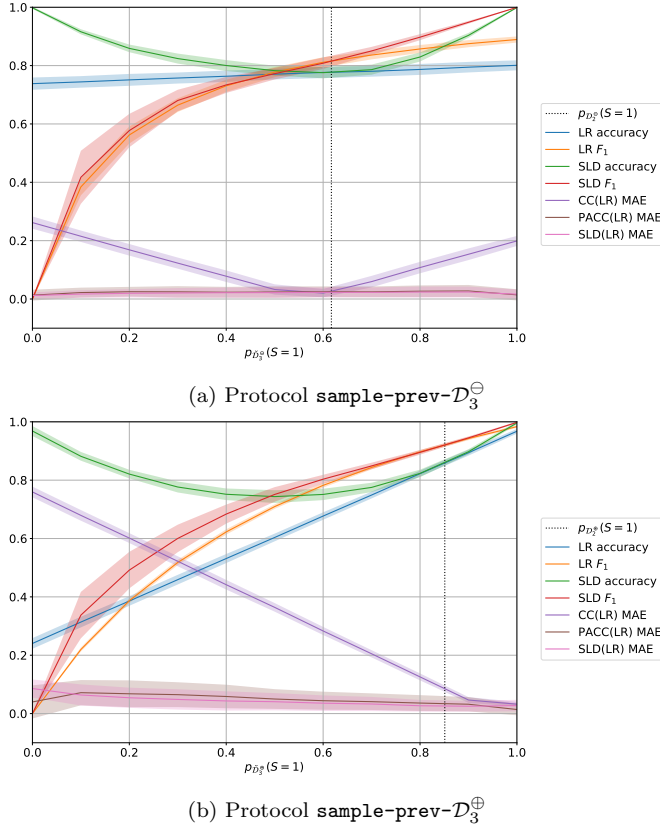


Fig. 8: Performance of CC, SLD and PACC on the Adult dataset when used for quantification (MAE – lower is better) and classification (F_1 , accuracy – higher is better) under protocol **sample-prev- \mathcal{D}_3** . The classification performance of PACC is equivalent to that of CC (both equal to the performance of the underlying LR), and we thus omit it for readability.

6 Related work

6.1 Fairness under unawareness of sensitive attributes

Several fairness criteria have been proposed in the machine learning literature, typically requiring equalization of some conditional or marginal property of the joint distribution of the sensitive variable S , ground truth Y , and classifier estimate \hat{Y} (Dwork et al., 2012; Hardt et al., 2016; Narayanan, 2018). Unavailability of the sensitive attribute poses a major challenge for internal and external fairness audits under any of these criteria. When the sensitive attribute is unknown, it is sometimes possible to seek expert advice for its annotation (Buolamwini and Gebru, 2018). Alternatively, disclosure proce-

dures have been proposed for subjects to provide their sensitive attributes to a trusted third party (Veale and Binns, 2017) or to share them in encrypted form (Kilbertus et al., 2018). Another line of research, closely related to our work, studies the problem of reliably estimating measures of group fairness with no access to sensitive attributes via proxy variables (Awasthi et al., 2021; Chen et al., 2019; Kallus et al., 2020).

Chen et al. (2019) study the problem of estimating the demographic parity of a classifier, defined in terms of the distribution of \hat{Y} conditional on S , exploiting non-sensitive variables X as proxies to infer the sensitive variable S . They characterize the limitations of a CC-based approach and propose a *weighted estimator* with better convergence properties, closely related to PCC. The authors stress the tendency of CC to exaggerate disparities as a key problem. In this work, we show extensive empirical evidence of this phenomenon and adapt different approaches from the quantification literature to overcome this limitation. Kallus et al. (2020) study the identifiability of a classifier’s demographic parity in a setting with access to a primary dataset involving (\hat{Y}, Z) and an auxiliary dataset involving (S, Z) , where Z is a generic set of proxy variables, potentially disjoint from X . They show that reliably estimating the demographic parity of a classifier issuing predictions \hat{Y} when Z is not highly informative with respect to either \hat{Y} or S is infeasible. Moreover, they provide upper and lower bounds for the true value of the estimand in a setting where the primary and auxiliary datasets are drawn from marginalizations of a common joint distribution. In a similar setting, Awasthi et al. (2021) characterize the structure of the best classifier for sensitive attributes when the final estimand is a classifier’s disparity in true positive rates across protected groups. They show that the test accuracy of the attribute classifier and its performance as an estimator of the true positive rate disparity is not necessarily correlated.

Our work expands on this prior art, making realistic assumptions for an internal audit of demographic parity. We study the problem of estimating the demographic disparity of a classifier h on production data, allowing for different types of dataset shift between its training set, its deployment set, and a small auxiliary set with information on the sensitive attribute. We leverage techniques from quantification learning, directly aimed at group-level estimates, which are reliable even when the underlying sensitive attribute classifier performs poorly. Moreover, we show that the quantification and classification objectives can be successfully decoupled.

6.2 Quantification and fairness

The application of quantification approaches in algorithmic fairness research is not entirely new. Biswas and Mukherjee (2021) study the problem of enforcing fair classification under prior probability shift, potentially affecting different demographic groups at different rates. They define a notion of fairness based on proportionality between the prevalence of positives in a protected group

$S = s$ and the group-specific acceptance rate of a classifier issuing predictions \hat{Y} . This notion, called Proportional Equality, is defined by the quantity $PE = \left| \frac{\Pr(Y=\oplus|S=1)}{\Pr(Y=\oplus|S=0)} - \frac{\Pr(\hat{Y}=\oplus|S=1)}{\Pr(\hat{Y}=\oplus|S=0)} \right|$ computed on a test set \mathcal{D} , where low values of PE correspond to fairer predictions \hat{Y} . In the presence of distribution drift between training and testing conditions, the true group-specific prevalences $\Pr(Y = \oplus|S = 1)$ and $\Pr(Y = \oplus|S = 0)$ are unknown. The authors employ a PCC-based quantifier to estimate these prevalence values. PCC is embedded within a wider pipeline called CAPE, combining sampling, ensemble and quantification techniques to provide fair predictions.

In other words, prior work applying quantification to problems of algorithmic fairness concentrates on *ensuring* fairness of classifiers under unawareness of *target labels*. Our work, on the other hand, is aimed at *measuring* fairness under unawareness of *sensitive attributes*.

7 Discussion and conclusion

Measuring the differential impact of models on groups of individuals is important to understand their effects in the real world and their tendency to encode and reinforce divisions and privilege across sensitive attributes. Unfortunately, in practice, demographic attributes are often unavailable. In this work, we have taken the perspective of responsible practitioners, interested in internal fairness audits of production models. We have tackled the problem of measuring group fairness under unawareness of sensitive attributes by applying ad-hoc approaches from the quantification learning literature. These methods are specifically designed for group-level estimation rather than individual-level classification. Since practitioners who try to measure fairness under unawareness are precisely interested in group-level estimates, it is useful for the fairness and quantification communities to exchange lessons.

We have studied the problem of estimating a classifier’s demographic disparity at deployment under unawareness of sensitive attributes, with access to a disjoint auxiliary set of data for which demographic information is available. Drawing from the algorithmic fairness literature, we have identified five factors of import for this problem, associating each of them with a formal evaluation protocol. These factors mirror challenges in real-world applications, including dataset shift and variable cardinality for auxiliary datasets comprising demographic information. We have tested five quantification methods under every protocol, comparing them against the naïve Classify-and-Count (CC) method, which represents the default approach for practitioners unaware of quantification. Each quantification approach was shown to outperform CC under most combinations of 5 protocols, 3 datasets, and 2 underlying learners. Moreover, we have shown a simple approach to integrate quantification methods into existing machine learning pipelines with little orchestration effort, and demonstrated the importance of each component through an ablation study.

Finally, we have considered the problem of model misuse to infer demographic characteristics at an individual level, which represents a concern when

developing models to measure group fairness via proxy attributes. Through a dedicated set of experiments, we have shown that it is possible to obtain precise estimates of demographic disparity from methods that have poor classification performance. This is a positive result for decoupling these two objectives, which should help deter from the exploitation of these models for individual-level inference.

Future work may require a deeper study of the relation between classification and quantification performance, and the extent to which these two objectives may be decoupled. It would be interesting to especially target decoupling through learners aimed at maximizing quantification performance subject to a low classification performance constraint. Another important avenue for future work is the study of confidence intervals for estimates of demographic disparity provided by methods of quantification learning. An indication of confidence for point estimates of group fairness may be invaluable for a practitioner arguing for resources and attention to the disparate effects of a machine learning system on different populations.

Acknowledgments

The work by Alessandro Fabris was supported by MIUR (Italian Minister for Education) under the “Departments of Excellence” initiative (Law 232/2016). The work by Andrea Esuli, Alejandro Moreo, and Fabrizio Sebastiani has been supported by the SOBIGDATA++ project, funded by the European Commission (Grant 871042) under the H2020 Programme INFRAIA-2019-1, and by the AI4MEDIA project, funded by the European Commission (Grant 951911) under the H2020 Programme ICT-48-2020. The authors’ opinions do not necessarily reflect those of the European Commission.

References

- Amazon (2021) Amazon SageMaker developer guide: Conditional demographic disparity in predicted labels (CDDPL). URL <https://amzn.to/3rb8JkY>
- Andriotis A, Ensign RL (2015) US Government uses race test for \$80 million in payments. *The Wall Street Journal*, October 29, 2015, URL <https://on.wsj.com/36Bs9Gs>
- Andrus M, Spitzer E, Brown J, Xiang A (2021) What we can’t measure, we can’t understand: Challenges to demographic data procurement in the pursuit of fairness. In: *Proceedings of the 4th ACM Conference on Fairness, Accountability, and Transparency (FAccT 2021)*, Toronto, CA, pp 249–260
- Angwin J, Larson J, Mattu S, Kirchner L (2016) Machine bias. ProPublica, May 23, 2016, URL <https://bit.ly/36EeQoJ>
- Awasthi P, Kleindessner M, Morgenstern J (2020) Equalized odds postprocessing under imperfect group information. In: *Proceedings of the 23rd International Conference on Artificial Intelligence and Statistics (AISTATS 2020)*, Virtual Event, pp 1770–1780
- Awasthi P, Beutel A, Kleindessner M, Morgenstern J, Wang X (2021) Evaluating fairness of machine learning models under uncertain and incomplete information. In: *Proceedings of the 4th ACM Conference on Fairness, Accountability, and Transparency (FAccT 2021)*, Toronto, CA, pp 206–214
- Baker DW, Cameron KA, Feinglass J, Georgas P, Foster S, Pierce D, Thompson JA, Hasnain-Wynia R (2005) Patients’ attitudes toward health care providers collecting information about their race and ethnicity. *Journal of General Internal Medicine* 20(10):895–900
- Barenstein M (2019) Propublica’s compas data revisited. arXiv preprint arXiv:190604711
- Barocas S, Hardt M, Narayanan A (2019) Fairness and machine learning. fairmlbook.org, URL <http://www.fairmlbook.org>
- Bella A, Ferri C, Hernández-Orallo J, Ramírez-Quintana MJ (2010) Quantification via probability estimators. In: *Proceedings of the 11th IEEE International Conference on Data Mining (ICDM 2010)*, Sydney, AU, pp 737–742, DOI 10.1109/icdm.2010.75
- Bertrand M, Mullainathan S (2004) Are Emily and Greg more employable than Lakisha and Jamal? A field experiment on labor market discrimination. *American Economic Review* 94(4):991–1013
- Beutel A, Chen J, Doshi T, Qian H, Wei L, Wu Y, Heldt L, Zhao Z, Hong L, Chi EH, Goodrow C (2019a) Fairness in recommendation ranking through pairwise comparisons. In: *Proceedings of the 25th ACM International Conference on Knowledge Discovery and Data Mining (KDD 2019)*, Anchorage, US, pp 2212–2220, DOI 10.1145/3292500.3330745
- Beutel A, Chen J, Doshi T, Qian H, Woodruff A, Luu C, Kreitmann P, Bischof J, Chi EH (2019b) Putting fairness principles into practice: Challenges, metrics, and improvements. In: *Proceedings of the 2nd AAAI/ACM Conference on AI, Ethics, and Society (AIES 2019)*, Honolulu, US, p 453–459, DOI 10.1145/3306618.3314234

- Biswas A, Mukherjee S (2021) Ensuring fairness under prior probability shifts. In: Proceedings of the 2021 AAAI/ACM Conference on AI, Ethics, and Society, Association for Computing Machinery, New York, NY, USA, AIES '21, p 414–424, DOI 10.1145/3461702.3462596, URL <https://doi.org/10.1145/3461702.3462596>
- Bogen M, Rieke A, Ahmed S (2020) Awareness in practice: Tensions in access to sensitive attribute data for antidiscrimination. In: Proceedings of the 3rd ACM Conference on Fairness, Accountability, and Transparency (FAT* 2020), Barcelona, ES, pp 492–500
- Buolamwini J, Gebru T (2018) Gender shades: Intersectional accuracy disparities in commercial gender classification. In: Proceedings of the 1st ACM Conference on Fairness, Accountability and Transparency (FAT* 2018), New York, US, pp 77–91
- Chen J, Kallus N, Mao X, Svacha G, Udell M (2019) Fairness under unawareness: Assessing disparity when protected class is unobserved. In: Proceedings of the 2nd ACM Conference on Fairness, Accountability, and Transparency (FAT* 2019), Atlanta, US, p 339–348
- Coston A, Ramamurthy KN, Wei D, Varshney KR, Speakman S, Mustahsan Z, Chakraborty S (2019) Fair transfer learning with missing protected attributes. In: Proceedings of the 2nd AAAI/ACM Conference on AI, Ethics, and Society (AIES 2019), Honolulu, US, pp 91–98, DOI 10.1145/3306618.3314236
- Cvencek D, Meltzoff AN, Greenwald AG (2011) Math-gender stereotypes in elementary school children. *Child Development* 82(3):766–779
- Ditzler G, Roveri M, Alippi C, Polikar R (2015) Learning in nonstationary environments: A survey. *IEEE Computational Intelligence* 10(4):12–25, DOI 10.1109/MCI.2015.2471196
- Donini M, Oneto L, Ben-David S, Shawe-Taylor JS, Pontil M (2018) Empirical risk minimization under fairness constraints. In: Proceedings of the 32nd Annual Conference on Neural Information Processing Systems (NeurIPS 2018), Montreal, CA, pp 2791–2801
- Dwork C, Hardt M, Pitassi T, Reingold O, Zemel R (2012) Fairness through awareness. In: Proceedings of the 3rd Innovations in Theoretical Computer Science Conference (ITCS 2012), Cambridge, US, pp 214–226, DOI 10.1145/2090236.2090255
- Ellemers N (2018) Gender stereotypes. *Annual Review of Psychology* 69(1):275–298
- Elliott MN, Morrison PA, Fremont A, McCaffrey DF, Pantoja P, Lurie N (2009) Using the Census Bureau’s surname list to improve estimates of race/ethnicity and associated disparities. *Health Services and Outcomes Research Methodology* 9(2):69–83
- Fernandes Vaz A, Izbicki R, Bassi Stern R (2019) Quantification under prior probability shift: The ratio estimator and its extensions. *Journal of Machine Learning Research* 20:79:1–79:33
- Fogliato R, Chouldechova A, G’Sell M (2020) Fairness evaluation in presence of biased noisy labels. In: Proceedings of the 23rd International Conference

- on Artificial Intelligence and Statistics (AISTATS 2020), Virtual Event, pp 2325–2336
- Fogliato R, Xiang A, Lipton Z, Nagin D, Chouldechova A (2021) On the validity of arrest as a proxy for offense: Race and the likelihood of arrest for violent crimes. In: Proceedings of the 4th AAAI/ACM Conference on AI, Ethics, and Society (AIES 2021), Virtual Event, pp 100–111, DOI 10.1145/3461702.3462538
- Forman G (2008) Quantifying counts and costs via classification. *Data Mining and Knowledge Discovery* 17(2):164–206, DOI 10.1007/s10618-008-0097-y
- Galdon Clavell G, Martín Zamorano M, Castillo C, Smith O, Matic A (2020) Auditing algorithms: On lessons learned and the risks of data minimization. In: Proceedings of the 3rd AAAI/ACM Conference on AI, Ethics, and Society (AIES 2020), New York, US, pp 265–271, DOI 10.1145/3375627.3375852
- Geyik SC, Ambler S, Kenthapadi K (2019) Fairness-aware ranking in search and recommendation systems with application to LinkedIn talent search. In: Proceedings of the 25th ACM International Conference on Knowledge Discovery and Data Mining (KDD 2019), Anchorage, US, pp 2221–2231, DOI 10.1145/3292500.3330691
- Gianfrancesco MA, Tamang S, Yazdany J, Schmajuk G (2018) Potential biases in machine learning algorithms using electronic health record data. *JAMA Internal Medicine* 178(11):1544–1547
- González P, Castaño A, Chawla NV, del Coz JJ (2017) A review on quantification learning. *ACM Computing Surveys* 50(5):74:1–74:40, DOI 10.1145/3117807
- González-Castro V, Alaiz-Rodríguez R, Alegre E (2013) Class distribution estimation based on the Hellinger distance. *Information Sciences* 218:146–164, DOI 10.1016/j.ins.2012.05.028
- Hardt M, Price E, Srebro N (2016) Equality of opportunity in supervised learning. In: Proceedings of the 29th Annual Conference on Neural Information Processing Systems (NIPS 2016), Barcelona, ES, pp 3323–3331
- Hashimoto T, Srivastava M, Namkoong H, Liang P (2018) Fairness without demographics in repeated loss minimization. In: Proceedings of the 35th International Conference on Machine Learning (ICML 2018), Stockholm, SE, pp 1929–1938
- Hasnain-Wynia R, Baker DW (2006) Obtaining data on patient race, ethnicity, and primary language in health care organizations: Current challenges and proposed solutions. *Health Services Research* 41(4p1):1501–1518, DOI 10.1111/j.1475-6773.2006.00552.x.
- He Y, Burghardt K, Lerman K (2020) A geometric solution to fair representations. In: Proceedings of the AAAI/ACM Conference on AI, Ethics, and Society (AIES 2020), New York, US, pp 279–285, DOI 10.1145/3375627.3375864
- Holmes MD, Smith BW, Freng AB, Muñoz EA (2008) Minority threat, crime control, and police resource allocation in the southwestern United States. *Crime and Delinquency* 54(1):128–152, DOI 10.1177/0011128707309718

- Holstein K, Wortman Vaughan J, Daumé III H, Dudik M, Wallach H (2019) Improving fairness in machine learning systems: What do industry practitioners need? In: Proceedings of the ACM Conference on Human Factors in Computing Systems (CHI 2019), Glasgow, UK, pp 1–16
- Hu L, Immorlica N, Vaughan JW (2019) The disparate effects of strategic manipulation. In: Proceedings of the 2nd ACM Conference on Fairness, Accountability, and Transparency (FAT* 2019), Atlanta, US, pp 259–268, DOI 10.1145/3287560.3287597
- Kallus N, Zhou A (2018) Residual unfairness in fair machine learning from prejudiced data. In: Proceedings of the 35th International Conference on Machine Learning (ICML 2018), Stockholm, SE, pp 2439–2448
- Kallus N, Zhou A (2021) Fairness, welfare, and equity in personalized pricing. In: Proceedings of the 4th ACM Conference on Fairness, Accountability, and Transparency (FAccT 2021), Toronto, CA, pp 296–314, DOI 10.1145/3442188.3445895
- Kallus N, Mao X, Zhou A (2020) Assessing algorithmic fairness with unobserved protected class using data combination. In: Proceedings of the 3rd Conference on Fairness, Accountability, and Transparency (FAT* 2020), Barcelona, ES, p 110
- Keyes O (2018) The misgendering machines: Trans/hci implications of automatic gender recognition. Proceedings of the ACM on Human-Computer Interaction 2(CSCW):88:1–88:22, DOI 10.1145/3274357
- Kilbertus N, Gascon A, Kusner M, Veale M, Gummadi K, Weller A (2018) Blind justice: Fairness with encrypted sensitive attributes. In: Proceedings of the 35th International Conference on Machine Learning (ICML 2018), Stockholm, SE, pp 2630–2639
- Koren JR (2016) Feds use Rand formula to spot discrimination. the GOP calls it junk science. Los Angeles Times, August 23, 2016, URL <https://lat.ms/3r8naXb>
- Larson J, Mattu S, Kirchner L, Angwin J (2016) How we analyzed the COMPAS recidivism algorithm. ProPublica, May 23, 2016, URL <https://bit.ly/2T8wduy>
- Lindberg SM, Hyde JS, Petersen JL, Linn MC (2010) New trends in gender and mathematics performance: A meta-analysis. Psychological Bulletin 136(6):1123–1135, DOI 10.1037/a0021276
- Lipton Z, McAuley J, Chouldechova A (2018) Does mitigating ML’s impact disparity require treatment disparity? In: Proceedings of the 32nd Annual Conference on Neural Information Processing Systems (NeurIPS 2018), Montreal, CA, pp 8136–8146
- Malinin A, Band N, Chesnokov G, Gal Y, Gales MJ, Noskov A, Ploskonosov A, Prokhorenkova L, Provilkov I, Raina V, et al. (2021) Shifts: A dataset of real distributional shift across multiple large-scale tasks. arXiv preprint arXiv:210707455
- Mansoury M, Abdollahpouri H, Pechenizkiy M, Mobasher B, Burke R (2020) Feedback loop and bias amplification in recommender systems. In: Proceedings of the 29th ACM International Conference on Information and

- Knowledge Management (CIKM 2020), Virtual Event, pp 2145–2148, DOI 10.1145/3340531.3412152
- McLemore KA (2015) Experiences with misgendering: Identity misclassification of transgender spectrum individuals. *Self and Identity* 14(1):51–74
- Mehrotra A, Celis LE (2021) Mitigating bias in set selection with noisy protected attributes. In: *Proceedings of the 4th ACM Conference on Fairness, Accountability, and Transparency (FAccT 2021)*, Toronto, CA, pp 237–248, DOI 10.1145/3442188.3445887
- Moreno-Torres JG, Raeder T, Alaiz-Rodríguez R, Chawla NV, Herrera F (2012) A unifying view on dataset shift in classification. *Pattern Recognition* 45(1):521–530, DOI 10.1016/j.patcog.2011.06.019
- Moreo A, Sebastiani F (2021a) Re-assessing the “classify and count” quantification method. In: *Proceedings of the 43rd European Conference on Information Retrieval (ECIR 2021)*, Lucca, IT, vol II, pp 75–91
- Moreo A, Sebastiani F (2021b) Tweet sentiment quantification: An experimental re-evaluation. *arXiv:2011.08091 [cs.CL]*
- Namaste V (2000) *Invisible lives: The erasure of transsexual and transgendered people*. University of Chicago Press, Chicago, US
- Narayanan A (2018) 21 fairness definitions and their politics. In: Tutorial presented at the 1st ACM Conference on Fairness, Accountability and Transparency (FAT* 2018), New York, US
- Nosek BA, Banaji MR, Greenwald AG (2002) Math=male, me=female, therefore math≠me. *Journal of Personality and Social Psychology* 83(1):44–59
- Obermeyer Z, Powers B, Vogeli C, Mullainathan S (2019) Dissecting racial bias in an algorithm used to manage the health of populations. *Science* 366(6464):447–453
- Platt JC (2000) Probabilistic outputs for support vector machines and comparison to regularized likelihood methods. In: Smola A, Bartlett P, Schölkopf B, Schuurmans D (eds) *Advances in Large Margin Classifiers*, The MIT Press, Cambridge, MA, pp 61–74
- ProPublica (2016) *Compas analysis github repository*. URL <https://github.com/propublica/compas-analysis>
- Raji ID, Smart A, White RN, Mitchell M, Gebru T, Hutchinson B, Smith-Loud J, Theron D, Barnes P (2020) Closing the AI accountability gap: Defining an end-to-end framework for internal algorithmic auditing. In: *Proceedings of the 3rd Conference on Fairness, Accountability, and Transparency (FAT* 2020)*, Barcelona, ES, pp 33–44
- Saerens M, Latinne P, Decaestecker C (2002) Adjusting the outputs of a classifier to new a priori probabilities: A simple procedure. *Neural Computation* 14(1):21–41, DOI 10.1162/089976602753284446
- Schouten B, Cobben F, Bethlehem J (2009) Indicators for the representativeness of survey response. *Survey Methodology* 35(1):101–113
- Schouten B, Bethlehem J, Beullens K, Kleven O, Loosveldt G, Luiten A, Rutar K, Shlomo N, Skinner C (2012) Evaluating, comparing, monitoring, and improving representativeness of survey response through R-indicators and partial R-indicators. *International Statistical Review* 80(3):382–399

- Selbst AD, Boyd D, Friedler SA, Venkatasubramanian S, Vertesi J (2019) Fairness and abstraction in sociotechnical systems. In: Proceedings of the 2nd ACM Conference on Fairness, Accountability, and Transparency (FAT* 2019), Atlanta, US, pp 59–68, DOI 10.1145/3287560.3287598
- Sindreu J (2021) Covid-19 wrecked the algorithms that set airfares, but they won't stay dumb. *The Wall Street Journal*, May 17, 2021, URL <https://on.wsj.com/2UQg1yQ>
- Singh H, Singh R, Mhasawade V, Chunara R (2021) Fairness violations and mitigation under covariate shift. In: Proceedings of the 4th ACM Conference on Fairness, Accountability, and Transparency (FAccT 2021), Toronto, CA, pp 3–13, DOI 10.1145/3442188.3445865
- Tsirtsis S, Tabibian B, Khajehnejad M, Singla A, Schölkopf B, Gomez-Rodriguez M (2019) Optimal decision making under strategic behavior. arXiv preprint arXiv:190509239
- Veale M, Binns R (2017) Fairer machine learning in the real world: Mitigating discrimination without collecting sensitive data. *Big Data and Society* 4(2):1–17, DOI 10.1177/2053951717743530
- Wachter S, Mittelstadt B, Russell C (2020) Why fairness cannot be automated: Bridging the gap between EU non-discrimination law and AI. *Computer Law and Security Review* 41, DOI 10.1016/j.clsr.2021.105567, article 105567
- Wang J, Liu Y, Levy C (2021) Fair classification with group-dependent label noise. In: Proceedings of the 4th ACM Conference on Fairness, Accountability, and Transparency (FAccT 2021), Toronto, CA, pp 526–536, DOI 10.1145/3442188.3445915
- Wilson C, Ghosh A, Jiang S, Mislove A, Baker L, Szary J, Trindel K, Polli F (2021) Building and auditing fair algorithms: A case study in candidate screening. In: Proceedings of the 4th ACM Conference on Fairness, Accountability, and Transparency (FAccT 2021), Toronto, CA, pp 666–677, DOI 10.1145/3442188.3445928
- Xie M, Lauritsen JL (2012) Racial context and crime reporting: A test of Black's stratification hypothesis. *Journal of Quantitative Criminology* 28(2):265–293
- Zafar MB, Valera I, Rognier MG, Gummadi KP (2017) Fairness constraints: Mechanisms for fair classification. In: Proceedings of the 20th International Conference on Artificial Intelligence and Statistics (AISTATS 2017), Fort Lauderdale, US, pp 962–970

Appendix A SVM-based quantification

In this appendix, we report the results of experiments, analogous to the ones in Sections 5.3-5.9, where quantifiers are wrapped around an SVM classifier rather than a LR classifier. The experimental protocols are summarized by Tables 9-13. The ablation study is depicted in Figures 9-13. Experiments on decoupling the quantification performance of a model from its classification performance are reported in Figures 14 and 15.

Table 9: Protocol **sample-prev- \mathcal{D}_1** with SVM-based classifier (Adult).

		MAE	MSE	$P(\text{AE} < 0.1)$	$P(\text{AE} < 0.2)$
Adult	CC(SVM)	0.123 \pm 0.043	0.017 \pm 0.009	0.253	0.993
	PCC(SVM)	0.007 \pm 0.005	0.000 \pm 0.000	1.000	1.000
	ACC(SVM)	0.030 \pm 0.027	0.002 \pm 0.005	0.982	0.998
	PACC(SVM)	0.019 \pm 0.014	0.001 \pm 0.001	1.000	1.000
	EMQ(SVM)	0.015 \pm 0.011	0.000 \pm 0.000	1.000	1.000
	HDy(SVM)	0.020 \pm 0.015	0.001 \pm 0.001	1.000	1.000
COMPAS	CC(SVM)	0.198 \pm 0.069	0.044 \pm 0.030	0.059	0.549
	PCC(SVM)	0.026 \pm 0.018	0.001 \pm 0.001	1.000	1.000
	ACC(SVM)	0.277 \pm 0.196	0.115 \pm 0.158	0.190	0.401
	PACC(SVM)	0.190 \pm 0.162	0.062 \pm 0.111	0.351	0.619
	EMQ(SVM)	0.157 \pm 0.157	0.049 \pm 0.105	0.447	0.758
	HDy(SVM)	0.101 \pm 0.079	0.016 \pm 0.025	0.575	0.882
CreditCard	CC(SVM)	0.069 \pm 0.044	0.007 \pm 0.008	0.769	0.994
	PCC(SVM)	0.012 \pm 0.009	0.000 \pm 0.000	1.000	1.000
	ACC(SVM)	0.199 \pm 0.157	0.064 \pm 0.098	0.321	0.588
	PACC(SVM)	0.145 \pm 0.117	0.035 \pm 0.056	0.435	0.741
	EMQ(SVM)	0.122 \pm 0.099	0.025 \pm 0.038	0.508	0.802
	HDy(SVM)	0.085 \pm 0.066	0.012 \pm 0.017	0.659	0.937

Table 10: Protocol **flip-prev- \mathcal{D}_1** with SVM-based classifier (Adult).

		MAE	MSE	$P(\text{AE} < 0.1)$	$P(\text{AE} < 0.2)$
Adult	CC(SVM)	0.153 \pm 0.076	0.029 \pm 0.023	0.271	0.689
	PCC(SVM)	0.007 \pm 0.005	0.000 \pm 0.000	1.000	1.000
	ACC(SVM)	0.027 \pm 0.024	0.001 \pm 0.003	0.985	0.999
	PACC(SVM)	0.019 \pm 0.015	0.001 \pm 0.001	1.000	1.000
	EMQ(SVM)	0.015 \pm 0.012	0.000 \pm 0.001	1.000	1.000
	HDy(SVM)	0.021 \pm 0.017	0.001 \pm 0.001	0.999	1.000
COMPAS	CC(SVM)	0.247 \pm 0.091	0.069 \pm 0.048	0.041	0.314
	PCC(SVM)	0.026 \pm 0.019	0.001 \pm 0.001	0.998	1.000
	ACC(SVM)	0.289 \pm 0.197	0.122 \pm 0.162	0.174	0.358
	PACC(SVM)	0.191 \pm 0.158	0.061 \pm 0.103	0.348	0.616
	EMQ(SVM)	0.148 \pm 0.135	0.040 \pm 0.081	0.458	0.756
	HDy(SVM)	0.100 \pm 0.079	0.016 \pm 0.026	0.575	0.891
CreditCard	CC(SVM)	0.056 \pm 0.039	0.005 \pm 0.006	0.854	0.999
	PCC(SVM)	0.011 \pm 0.009	0.000 \pm 0.000	1.000	1.000
	ACC(SVM)	0.201 \pm 0.159	0.066 \pm 0.098	0.316	0.586
	PACC(SVM)	0.136 \pm 0.106	0.030 \pm 0.045	0.449	0.768
	EMQ(SVM)	0.109 \pm 0.088	0.020 \pm 0.031	0.558	0.853
	HDy(SVM)	0.086 \pm 0.064	0.011 \pm 0.016	0.644	0.940

Table 11: Protocol **sample-size- \mathcal{D}_2** with SVM-based classifier (Adult).

		MAE	MSE	$P(\text{AE} < 0.1)$	$P(\text{AE} < 0.2)$
Adult	CC(SVM)	0.127 \pm 0.030	0.017 \pm 0.007	0.180	1.000
	PCC(SVM)	0.012 \pm 0.011	0.000 \pm 0.001	1.000	1.000
	ACC(SVM)	0.080 \pm 0.119	0.021 \pm 0.091	0.776	0.939
	PACC(SVM)	0.048 \pm 0.062	0.006 \pm 0.032	0.887	0.975
	EMQ(SVM)	0.038 \pm 0.052	0.004 \pm 0.020	0.921	0.981
	HDy(SVM)	0.037 \pm 0.030	0.002 \pm 0.004	0.954	1.000
COMPAS	CC(SVM)	0.210 \pm 0.059	0.047 \pm 0.028	0.011	0.494
	PCC(SVM)	0.028 \pm 0.019	0.001 \pm 0.001	1.000	1.000
	ACC(SVM)	0.309 \pm 0.215	0.142 \pm 0.182	0.165	0.357
	PACC(SVM)	0.243 \pm 0.205	0.101 \pm 0.164	0.270	0.525
	EMQ(SVM)	0.204 \pm 0.174	0.072 \pm 0.122	0.330	0.603
	HDy(SVM)	0.115 \pm 0.088	0.021 \pm 0.031	0.514	0.843
CreditCard	CC(SVM)	0.113 \pm 0.059	0.016 \pm 0.016	0.429	0.919
	PCC(SVM)	0.021 \pm 0.017	0.001 \pm 0.001	0.999	1.000
	ACC(SVM)	0.328 \pm 0.259	0.175 \pm 0.242	0.233	0.394
	PACC(SVM)	0.322 \pm 0.249	0.165 \pm 0.225	0.223	0.395
	EMQ(SVM)	0.262 \pm 0.225	0.119 \pm 0.184	0.303	0.501
	HDy(SVM)	0.122 \pm 0.100	0.025 \pm 0.042	0.507	0.811

Table 12: Protocol **sample-prev- \mathcal{D}_2** with SVM-based classifier (Adult).

		MAE	MSE	$P(\text{AE} < 0.1)$	$P(\text{AE} < 0.2)$
Adult	CC(SVM)	0.235 \pm 0.170	0.084 \pm 0.108	0.271	0.491
	PCC(SVM)	0.253 \pm 0.188	0.099 \pm 0.131	0.246	0.459
	ACC(SVM)	0.140 \pm 0.146	0.041 \pm 0.107	0.496	0.795
	PACC(SVM)	0.103 \pm 0.094	0.019 \pm 0.047	0.596	0.885
	EMQ(SVM)	0.088 \pm 0.082	0.014 \pm 0.033	0.665	0.924
	HDy(SVM)	0.193 \pm 0.152	0.061 \pm 0.086	0.351	0.592
COMPAS	CC(SVM)	0.425 \pm 0.269	0.253 \pm 0.246	0.079	0.267
	PCC(SVM)	0.248 \pm 0.168	0.090 [‡] \pm 0.104	0.233	0.458
	ACC(SVM)	0.406 \pm 0.277	0.241 \pm 0.286	0.126	0.258
	PACC(SVM)	0.305 \pm 0.239	0.150 \pm 0.224	0.202	0.410
	EMQ(SVM)	0.248 \pm 0.215	0.107 \pm 0.183	0.279	0.524
	HDy(SVM)	0.236 \pm 0.179	0.088 \pm 0.121	0.273	0.510
CreditCard	CC(SVM)	0.384 \pm 0.257	0.214 \pm 0.219	0.131	0.320
	PCC(SVM)	0.233 \pm 0.146	0.076 \pm 0.077	0.228	0.444
	ACC(SVM)	0.436 \pm 0.316	0.290 \pm 0.326	0.191	0.299
	PACC(SVM)	0.439 \pm 0.322	0.296 \pm 0.336	0.195	0.299
	EMQ(SVM)	0.409 \pm 0.292	0.253 \pm 0.287	0.183	0.305
	HDy(SVM)	0.260 \pm 0.181	0.100 \pm 0.124	0.221	0.439

Table 13: Protocol **sample-prev- \mathcal{D}_3** with SVM-based classifier (Adult).

		MAE	MSE	$P(\text{AE} < 0.1)$	$P(\text{AE} < 0.2)$
Adult	CC(SVM)	0.315 \pm 0.258	0.166 \pm 0.228	0.233	0.433
	PCC(SVM)	0.260 \pm 0.195	0.106 \pm 0.138	0.242	0.456
	ACC(SVM)	0.080 \pm 0.070	0.011 \pm 0.021	0.705	0.935
	PACC(SVM)	0.049 \pm 0.039	0.004 \pm 0.006	0.892	0.997
	EMQ(SVM)	0.043 \pm 0.035	0.003 \pm 0.005	0.927	0.998
	HDy(SVM)	0.070 \pm 0.048	0.007 \pm 0.009	0.768	0.985
COMPAS	CC(SVM)	0.364 \pm 0.268	0.204 \pm 0.244	0.197	0.361
	PCC(SVM)	0.289 \pm 0.189	0.120 \pm 0.133	0.187	0.379
	ACC(SVM)	0.412 \pm 0.304	0.262 \pm 0.351	0.138	0.281
	PACC(SVM)	0.200 [‡] \pm 0.181	0.073 [‡] \pm 0.137	0.359	0.622
	EMQ(SVM)	0.197 \pm 0.177	0.070 \pm 0.122	0.371	0.635
	HDy(SVM)	0.224 \pm 0.167	0.078 \pm 0.108	0.276	0.520
CreditCard	CC(SVM)	0.276 \pm 0.178	0.108 \pm 0.118	0.196	0.387
	PCC(SVM)	0.280 \pm 0.170	0.107 \pm 0.106	0.184	0.368
	ACC(SVM)	0.299 \pm 0.227	0.141 \pm 0.201	0.213	0.400
	PACC(SVM)	0.231 \pm 0.178	0.085 \pm 0.123	0.276	0.515
	EMQ(SVM)	0.220 \pm 0.168	0.077 \pm 0.108	0.284	0.538
	HDy(SVM)	0.207 \pm 0.155	0.067 \pm 0.092	0.302	0.558

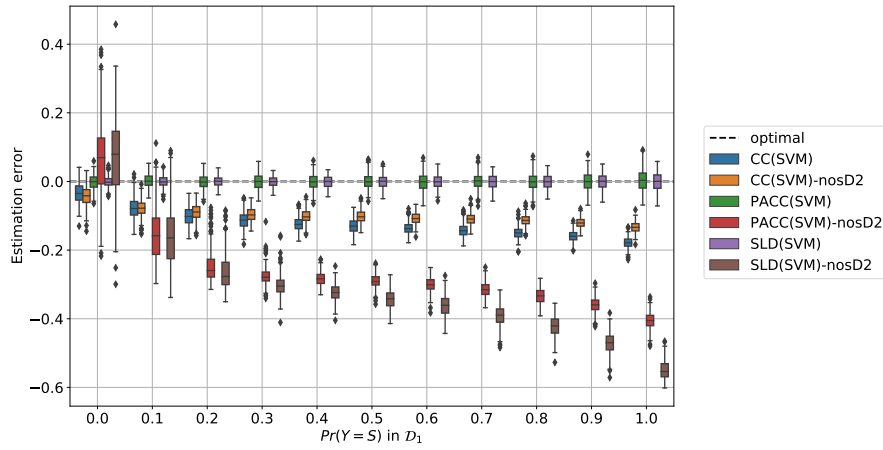


Fig. 9: Ablation study on the Adult dataset with SVM-based quantification for protocol **sample-prev- \mathcal{D}_1** .

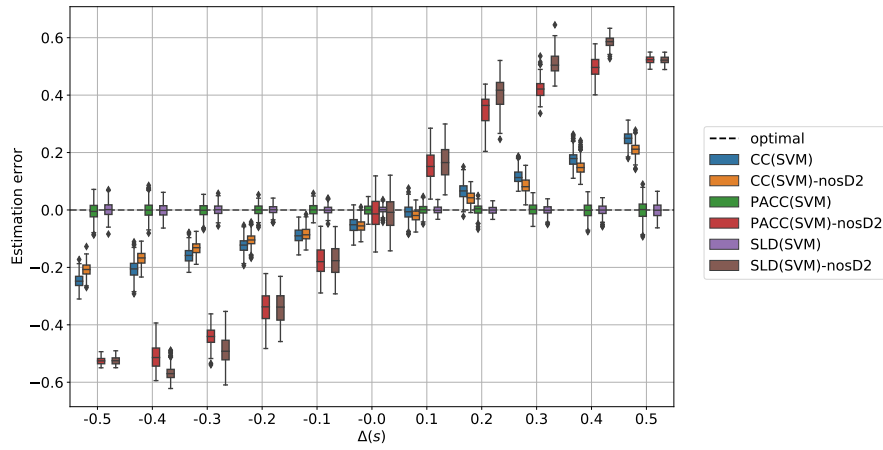


Fig. 10: Ablation study on the Adult dataset with SVM-based quantification for protocol **flip-prev- \mathcal{D}_1** .

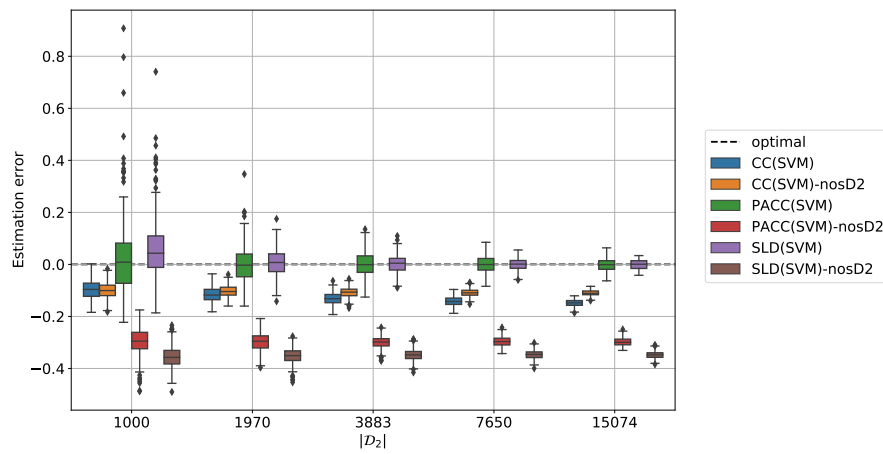


Fig. 11: Ablation study on the Adult dataset with SVM-based quantification for protocol **sample-size- \mathcal{D}_2** .

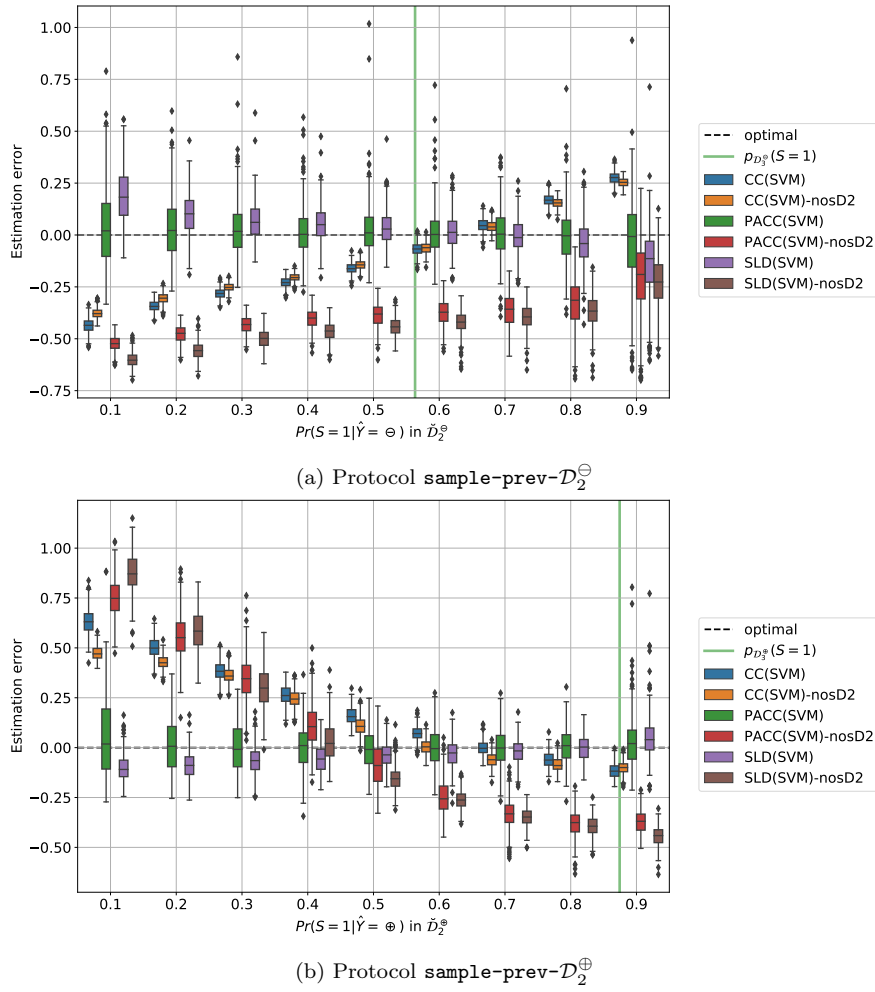


Fig. 12: Ablation study on the Adult dataset with SVM-based quantification for protocol **sample-prev- \mathcal{D}_2** .

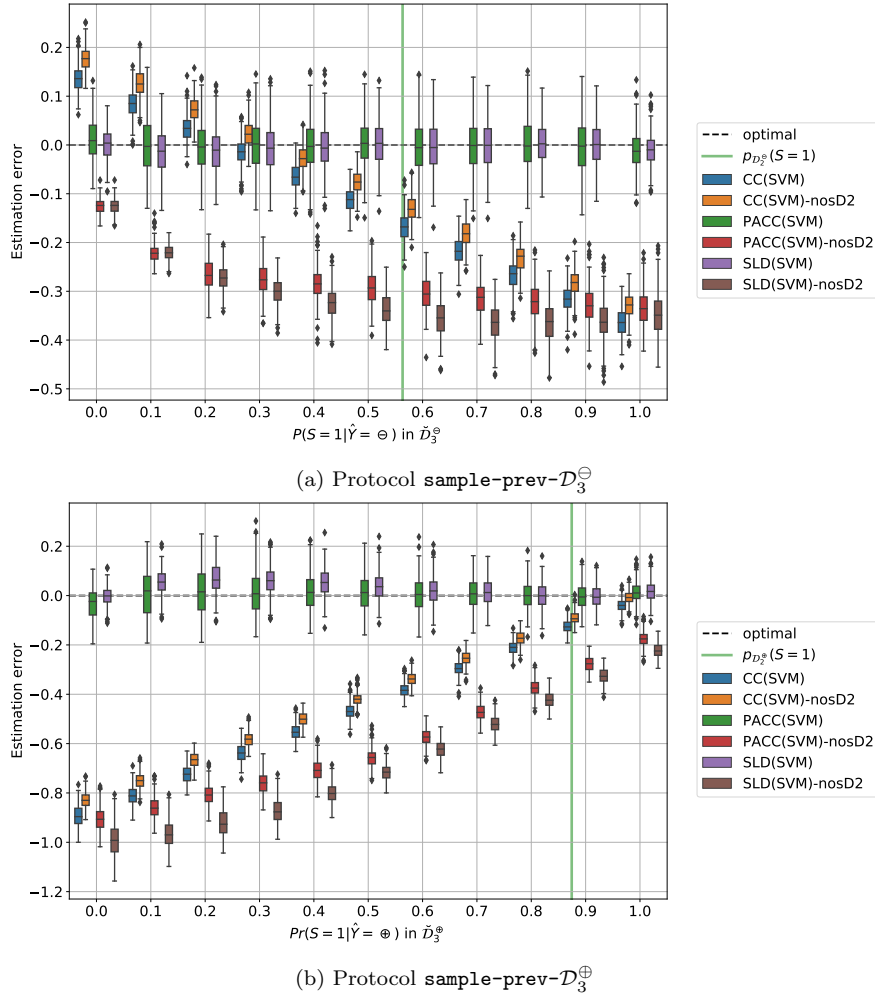


Fig. 13: Ablation study on the Adult dataset with SVM-based quantification for protocol $\text{sample-prev-}\mathcal{D}_3$.

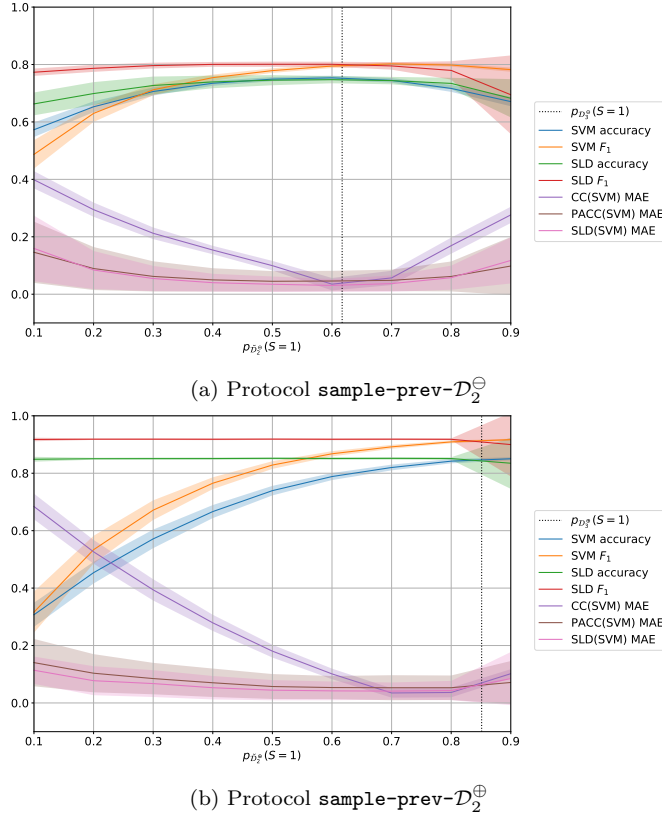


Fig. 14: Performance of SVM-based methods CC, SLD and PACC on the Adult dataset when used for quantification (MAE – lower is better) and classification (F_1 , accuracy – higher is better) under protocol **sample-prev- \mathcal{D}_2** . The classification performance of PACC is equivalent to that of CC (both equal to the performance of the underlying SVM), and we thus omit it for readability.

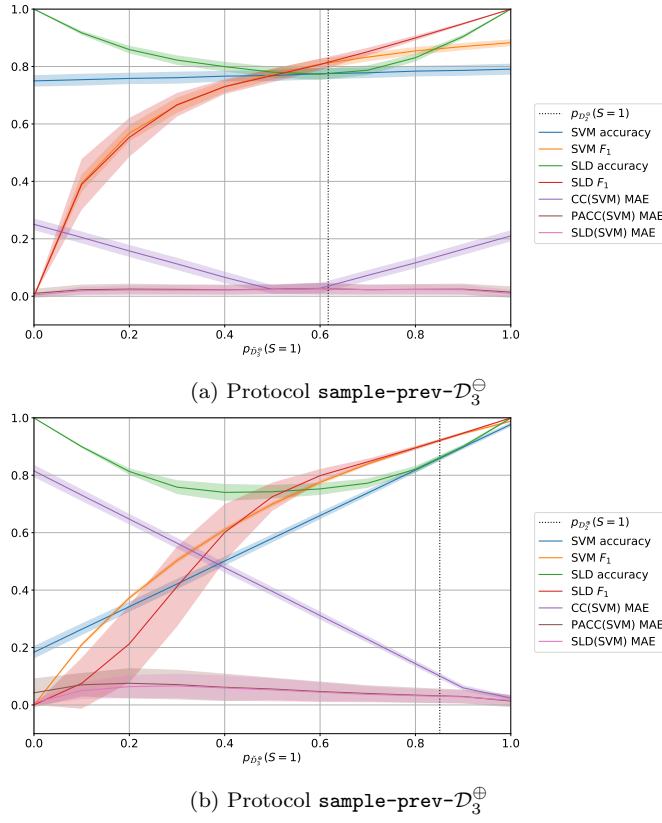


Fig. 15: Performance of SVM-based methods CC, SLD and PACC on the Adult dataset when used for quantification (MAE – lower is better) and classification (F_1 , accuracy – higher is better) under protocol **sample-prev- \mathcal{D}_3** . The classification performance of PACC is equivalent to that of CC (both equal to the performance of the underlying SVM), and we thus omit it for readability.